POLITECNICO DI MILANO

School of Industrial and Information Engineering

Master of Science in Telecommunication Engineering

Relay Facilitated Ultra Reliable and Low Latency Communication in UAV-assisted Wireless Cellular Systems

Supervisor: Prof. Maurizio Magarini

Thesis submission by,

Jayavathi Jayaraman
Matricola: 919233

Academic Year 2020-2021

Table of Contents

List of Figures

List of Tables

Acknowledgement

Foremost, I would like to express my sincere gratitude to my Prof. Maurizio Magarini for the continuous support for the research work, for his patience, availability, motivation, and enthusiasm. His assistance allowed me to think deeper about the practicality of those sophisticated formulas. I could not have imagined having a better advisor and mentor for my master's thesis.

It is my privilege to thank my friend Vishvanth Raja for his continuous support, encouragement. Indeed, without his support, I could have never been able to finish this dissertation.

I am thankful for all my friends and university colleagues, for their constant source of inspiration. Your presence is extremely valuable and highly appreciated.

Last, but not least, I am deeply thankful to my devoted parents Jayaraman and Pakiyavathi, to whom words cannot express how grateful I am, to my amazing sibling Sivabalan for their sustained encouragement, support, and unconditional love. Without your support I could have never been able to step on this stage.

Abstract

Ultra-reliable and low-latency communication (URLLC) is one of the key differentiators in the fifth generation (5G) network. Mission-critical applications require URLLC to support important use cases such as remote control of robots, vehicle-to-vehicle (V2V) communications, tactile internet, industrial automation, etc. URLLC is characterised by short packets that have strict latency and reliability constraints. As per the 3rd generation partnership project (3GPP) URLLC requirements, it is anticipated that the reliability of a transmission of a 32-byte packet must be at least 99.999% and the latency should be no more than 1 millisecond.

However, in any cellular network, the communication is largely dependent on fixed infrastructure (base stations), which could be critically disrupted in case of natural disasters such as floods, earthquakes, tsunamis or hurricanes. These disasters can cause the communication infrastructures, such as cell towers and Land Mobile Radio System (LMRS) repeaters, to become dysfunctional.

In such cases, there is a need to deploy a temporary communication infrastructure to surmount the lack of connectivity. Existing cloud and communication infrastructures are not designed to operate in such conditions. Recently, Unmanned Aerial Vehicle (UAV) assisted communication has attracted considerable attention as it provides wireless connectivity to devices in areas that lack infrastructure coverage. Such a technology has received considerable research interest due to its flexible deployment and the dominance of Line-of-Sight (LoS) links. In fact, UAVs provide superior performance by dynamically adjusting their state to best suit the communication needs. For example, the high altitude of UAVs allows for LoS communication that mitigates shadowing and signal blockage. Moreover, UAVs can act as flying relays between the transmitting and receiving devices.

However, with only one UAV deployed, it can be difficult to achieve the probability of LoS and network availability for critical URLLC applications, while keeping cost and system complexity requirements met. To harness the advantages of UAVs in these situations and minimize the drawbacks at the same time, an alternative solution is to deploy a multi-UAVs system, which could utilize the inter-connectivity to maintain uninterrupted communication with a ground control station.

Inspired from the paper, “UAV-Assisted Uplink Transmission for Ultra-reliable and Low-latency Communications” [1], I worked on improving the probability of LoS by having an additional UAV. I have explored the potential use of fixed relays to support URLLC in different types of environments such as Suburban, Urban, Dense urban, and High-rise urban. The key idea is to leverage better link qualities provided in UAV communication systems. As a main contribution of this work, I have worked on improving the characterized latency, reliability, and network availability of UAV communication systems.

In my thesis work, the main idea is to place a fixed UAV on the side of the rooftop of a building that acts as a relay to increase the probability of LoS between the transmitter and the main UAV that act as flying base station. Notably, a two-hop amplify and forward (AF) relay can provide significant improvements in the channel capacity, channel gain, as well as quality of service (QoS).

Numerical results have shown that the additional relayed UAV has increased the chance of LoS that increases the reliability and achievability. This is very important for critical and real-time applications.

Sommario

La comunicazione ultra affidabile e a bassa latenza (URLLC) è uno dei principali fattori di differenziazione nelle reti di quinta generazione (5G). Le applicazioni mission-critical richiedono che URLLC supporti importanti casi d'uso come il controllo remoto di robot, comunicazioni di topo veicolo-a-veicolo (V2V), Internet tattile, automazione industriale, ecc. URLLC è caratterizzato da pacchetti corti che hanno rigidi vincoli di latenza e affidabilità. In base ai requisiti URLLC del progetto di partnership di terza generazione (3GPP), si prevede che l'affidabilità di una trasmissione di un pacchetto a 32 byte deve essere almeno del 99,999% e la latenza non deve essere superiore a 1 millisecondi.

Tuttavia, in qualsiasi rete cellulare, la comunicazione dipende in gran parte dall'infrastruttura fissa (stazioni base), che potrebbe non essere disponibile nel caso di disastri naturali come inondazioni, terremoti, tsunami o uragani. Questi disastri possono causare il malfunzionamento delle infrastrutture di comunicazione, come le torri cellulari e i ripetitori del Land Mobile Radio System (LMRS).

In questi casi, è necessario implementare un'infrastruttura di comunicazione temporanea per superare la mancanza di connettività. Le infrastrutture cloud e di comunicazione esistenti non sono progettate per funzionare in tali condizioni. Recentemente, la comunicazione supportato da Unmanned Aerial Vehicle (UAV) ha suscitato un notevole interesse in quanto forniscono connettività wireless ai dispositivi in aree prive di copertura infrastrutturale. In particolare ha attirato interesse dal punto di vista della ricerca grazie alla sua flessibilità di implementazione e al predominio dei collegamenti radio in visibilità diretta (LoS).

Gli UAV forniscono prestazioni superiori regolando dinamicamente il loro stato per soddisfare al meglio le esigenze di comunicazione. Ad esempio, l'alta quota degli UAV consente la comunicazione LoS che mitiga le ombre e il blocco del segnale. Inoltre, gli UAV possono fungere da relè volanti tra i dispositivi di trasmissione e ricezione.

Tuttavia, con un solo UAV distribuito, può essere difficile ottenere la probabilità di LoS e disponibilità di rete per le applicazioni URLLC, mantenendo al contempo soddisfatti i requisiti di costo e complessità del sistema. Per sfruttare i vantaggi degli UAV in queste situazioni e contemporaneamente ridurre al minimo gli svantaggi, una soluzione alternativa è un sistema multi-UAV distribuito, che sfrutta l'interconnessione reciproca per mantenere una comunicazione continua con la stazione di controllo.

Prendendo spunto dall’articolo " UAV-Assisted Uplink Transmission for Ultra-reliable and Low-latency Communications " [1] come riferimento, ho lavorato per migliorare la probabilità di LoS con un relè fisso. Ho esplorato il potenziale utilizzo di relè fissi per supportare URLLC in diversi tipi di ambienti come suburbano, urbano, urbano denso e urbano a molti piani. L'idea chiave è sfruttare le migliori qualità di collegamento fornite nei sistemi di comunicazione UAV. Abbiamo caratterizzato la latenza, l'affidabilità e la disponibilità di rete dei sistemi di comunicazione UAV.

Nel mio lavoro di tesi, posizionando relè fisso sul contorno del tetto di un edificio è possibile migliorare la probabilità di LoS tra il trasmettitore e l'UAV principale. In particolare, il relè di tipo amplify and forward (AF) a due hop può fornire miglioramenti significativi nella capacità del collegamento, nel guadagno del canale e nella qualità del servizio (QoS).

I risultati numerici dimostrano che il relè fisso aggiuntivo migliora la possibilità di LoS, l'affidabilità e la praticabilità. Questo è molto importante per le applicazioni critiche che devono operare in tempo reale.

List of abbreviations

URLLC	Ultra-reliable and low latency communication
UAV	Unmanned aerial vehicle
LoS	Line-of-sight
PLoS	Probability of line-of-sight
NLoS	Non-line-of-sight
ATG	Air to ground communication
E2E	End to end delay
AF	Amplify and forward protocol
PER	Packet error rate
QoS	quality-of-service
M2M	Machine to machine communications
BS	Base station
AP	Access point
FIFO	First-in first-out
UL	Uplink
DL	Downlink
TTI	Transmission time interval
BER	Bit error rate
SNR	Signal to noise ratio
CNPC	Control and non-payload communication
UE	User equipment
G2G	Ground to ground communication
PDF	Probability density function
GPS	Global positioning system
3GPP	3rd generation partnership project
LAP	Low altitude platform
HAP	High altitude platform

FANET	Flying ad-hoc network
eMBB	enhanced Mobile broadband services
5G	Fifth generation
5G-ACIA	5G alliance for connected industries and automation
NR	New radio
LTE	Long-term evolution
SDU	Service data unit
RTT	Round trip time
HARQ	Hybrid automatic repeat request
MCS	Modulation and coding schemes
KPIs	Key performance indicators
ATC	Air traffic control
D2D	Device to device communication
MU	Mobile users
AWGN	Additive white gaussian noise
IBER	Information bit error rate
CSI	Channel state information
ITU	International telecommunication union
FAA	Federal aviation authority
NASA	National aeronautics and space administration
BLoS	Beyond-line-of-sight
BLER	Block error rate

1 Introduction

A growing number of mission-critical applications have stringent communication performance and reliability requirements. Communications with vehicles, high-speed trains, drones, and industrial robots are just a few examples of applications where wireless must meet either high reliability (for example, $<10^{-5}$ packet drop rate) or low latency (for example, ~1ms) requirements, or both at the same time. These applications frequently have strong security requirements, too. To meet all these requirements, 5G combines URLLC with enhanced Mobile Broadband (eMBB) services under a unified 5G air interface framework.

Unmanned Aerial Vehicles (UAV) in low-altitude platforms (LAP) has recently gained significant popularity as key enablers for rapidly deployable relief networks where coverage is provided by onboard radio heads. These platforms can deliver essential wireless communication for public safety agencies in remote areas or during the aftermath of natural disasters. Due to technical limitations, the number of deployable UAVs could be very low, especially during the chaotic aftermath hours of a disaster. This fact mandates full exploitation of each of the deployed UAVs by optimizing its altitude to provide the best possible coverage.

With reference to an emergency situation in an urban scenario, in my thesis work, the altitude of such platforms to provide maximum radio coverage on the ground when a fixed relay is used. The analysis shows that the optimal altitude is a function of the maximum allowed path LoS and the statistical parameters of the urban environment. I have considered a two-dimensional UAV-enabled scenario, where a transmitter needs to send command messages to a receiver in a multi-hazard area. In real-life scenarios, there might be many obstacles such as walls, buildings, any objects that act as thick cement/metal walls that block the information from the transmitter and the receiver. Hence, the channel gain between the ground transmitter and the flying receiver is weak and negligible and requires a UAV to stay above the obstacle to assist the transmission between them. I have studied the problem of jointly optimizing the block length and location for UAV-relay communication systems, where the amplify-and-forward (AF) protocol is considered.

However, an additional processing time is required for the AF mode, which may not apply to URLLC. Motivated by the above considerations, I have jointly optimized bandwidth and location to minimize the decoding error probability, where the relay is operating under the AF mode without the signal processing delay. The decoding error probability under short blocklength is adopted. From the analytical expressions, we can observe that the decoding error probability is a monotonically decreasing function of the SNR.

To meet the strict URLLC constraints, improvements can be made on each of the three dimensions: reducing latency directly; increasing reliability directly; and improving the throughput with resource-reuse, which can be transformed to improvements in low latency and high reliability. I have experimented how the performance changes when fixed relays are placed on the side of the rooftop of a building.

1.1 Content of the thesis

My thesis work is structured in different chapters as follows,

In Chapter 1, I have introduced the concept of 5G, given a detailed explanation of URLLC, applications of URLLC, channel coding rate in the finite blocklength regime and delay bound analysis.

In Chapter 2, I have gone through the background and key concepts of UAV such as classifications of UAV, UAV architecture, current technologies for UAV communications, key and challenging aspects and the regulation. I have given a brief introduction on the classical wireless channel.

In Chapter 3, I have discussed in detail on UAV-Assisted Uplink Transmission. It represents the scenario where a single UAV acts as an aerial base station aims to serve ground nodes in Uplink.

In Chapter 4, I have explained the proposed system model with the fixed relay on the side of the rooftop of a building and a flying UAV. I have quantified the benefits of adding the additional UAV that acts as a relay, showing that the reliability of air-to-ground communication link strongly benefits from the introduction of AF relay. Besides, I have collected data on the histogram of building heights in a particular location and worked on the localization to place the relay in order to increase the PLoS.

In Chapter 5, I have given the system and channel parameter assumptions, and compared the simulation results before and after the implementation of AF relay.

In Chapter 6, I have concluded the thesis work, with the scope and future work on this research.

2 A brief introduction to 5G and URLLC

The fifth generation (5G) of wireless cellular networks is the hottest topic in the telco industry in 2019 and early adopters are switching on their networks to provide a better user experience for consumers. It is expected to carry 1000 times more traffic while maintaining high reliability and supports three essential types of communications such as Enhanced Mobile Broadband (eMBB), Massive Machine Type Communication (mMTC), and Ultra-Reliable Low-Latency Communications (URLLC).

eMBB provides high data rates (up to several Gigabits per second) and offers enhanced coverage, well beyond that of previous generations. mMTC aims to provide wide area coverage and deep indoor penetration for thousands of IoT devices per square kilometer. This also supports the battery-saving low-energy operation. URLLC can facilitate highly critical applications with demanding requirements in terms of end-to-end (E2E) delay (in millisecond level), high reliability, and high availability.

For eMBB, 5G supports peak data rates of 20 Gb/s in the downlink and 10 Gb/s in the uplink. Such high data rates are enabled by a wide system bandwidth up to 400 MHz, massive MIMO, and high modulation orders such as 256 QAM. 5G intends to support operation at carrier frequencies below 1 GHz to up to 86 GHz and operates in both the licensed and license-exempt spectrum.

For mMTC usage, 5G provides connection densities far exceeding the requirement of 1 million devices per km^2 is achieved using efficient signalling. It also provides 20 dB coverage improvements and battery lifetimes exceeding 10 years are achieved by allowing extended discontinuous reception by extending the sleep mode of a device.

The development of 5G has not been through only to enlarge the broadband capabilities of mobile networks but also to provide advanced wireless connectivity for various sectors. The main focus is on machine-type communication and URLLC. It supports communication with high reliability, low latencies, and massive IoT connectivity. This paves the way for many use cases and applications in many various vertical domains such as automotive, healthcare, agriculture, energy & manufacturing sectors.

Figure 1 represents the architecture of the 5G network [23].

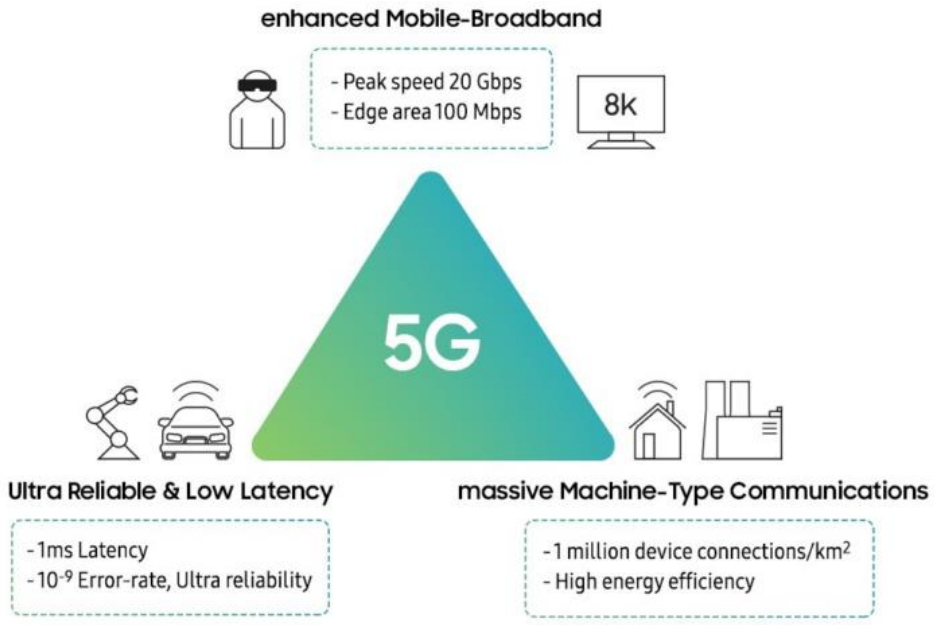

Figure 1 5G Architecture

2.1 Ultra-Reliable Low-Latency Communication

URLLC is a new service category in 5G to accommodate emerging services and applications having stringent latency and reliability requirements.

As per the 3rd generation partnership project (3GPP) URLLC requirements, it is anticipated that the reliability of a transmission of a 32-byte packet must be at least 99.999% and the latency should be at most 1ms. There is a huge number of potential URLLC applications that can be operated in either licensed or unlicensed bands. Most of the above applications have very strict quality-of-service (QoS) requirements on the end-to-end delay, reliability, and network availability. Due to path LoS, shadowing, and fast channel fading over wireless links, it is demanding to satisfy the QoS requirement of URLLC.

5G is being standardized in the form of two radio technology components: a novel radio interface denoted as new radio (NR), and long-term evolution (LTE). Low latency communication is enabled by the short new transmission slots which allow achieving faster uplink and downlink transmissions called mini slot for New Radio and short transmission time interval for LTE radio interfaces. Besides this, mechanisms to increase the reliability such as robust coding and modulation, and various diversity schemes have been developed following the LTE and NR designs [2].

Time and delay introduced at the transmitter while waiting for the next transmission opportunity are minimised by decreasing the transmission duration and the interval by some flexible adjustments. Higher reliability can be achieved by using robust modulation and coding schemes (MCS) and diversity techniques.

User plane latency is the measure of the time it takes to deliver a packet from the radio protocol layer Service Data Unit (SDU) ingress protocol to the radio protocol layer Service Data Unit (SDU) egress protocol via the radio interface in both Uplink and Downlink directions where neither device nor base station is restricted by discontinuous reception. Round trip time (RTT) includes user plane latency contributions, application processing times, and transport network delays [3].

Modem processing times, radio Transmission Time Interval (TTI), and an averaged contribution from Hybrid Automatic Repeat Request (HARQ) retransmissions all contribute to the user plane latency. 5G is expected to significantly reduce user plane latency to less than 1 millisecond. The shorter subframe duration for a reduced hybrid automatic repeat request (HARQ) transmission delay might reduce the delay.

By combining the header and data of short packets, the packet can be coded efficiently, and the data is delivered faster with less error. The users need to decode the combined packet, so energy efficiency is traded for very high reliability. There is also feasibility to achieve URLLC by using short transmission intervals without retransmission and equipping base stations (BSs) with large numbers of antennas to guarantee reliability via a spatial diversity gain.

Reliability is the success probability of transmitting some X bytes within the end-to-end delay. The latency can either be over one link (e.g., a side link), or over two links (e.g., between two user equipment (UE)) via the BS. Different from latency and reliability, which are the QoS required by each MU, availability is from the network perspective, and is another key performance metric for URLLC. Availability is defined as the probability that the network can support an MU with a target QoS requirement on latency and reliability.

To meet the rigorous constraints of future URLLC systems, the fundamental trade-off between error rate, throughput, and delay needs not only to be characterized but also to be met through the design of innovative new communication techniques. These include the design of short-packet coding, modulation and channel estimation, joint design of data and meta-data (control information), and optimization of wireless fading mitigation techniques for the latency-constrained context. The provision of timely status updates in sensing and actuation applications requires new design and analysis methods that incorporate queuing theory and communication theory [2].

2.2 Emerging URLLC Applications

There are a huge number of potential URLLC applications that can be operated in either licensed or unlicensed bands like Smart grid, Professional audio, Self-driving car, Industrial automation, Process automation, E-health, Augmented reality, Intelligent transport system, Vehicle-to-vehicle, Tactile Internet [3].

Some of the important applications of URLLC are represented in figure 2 [4].

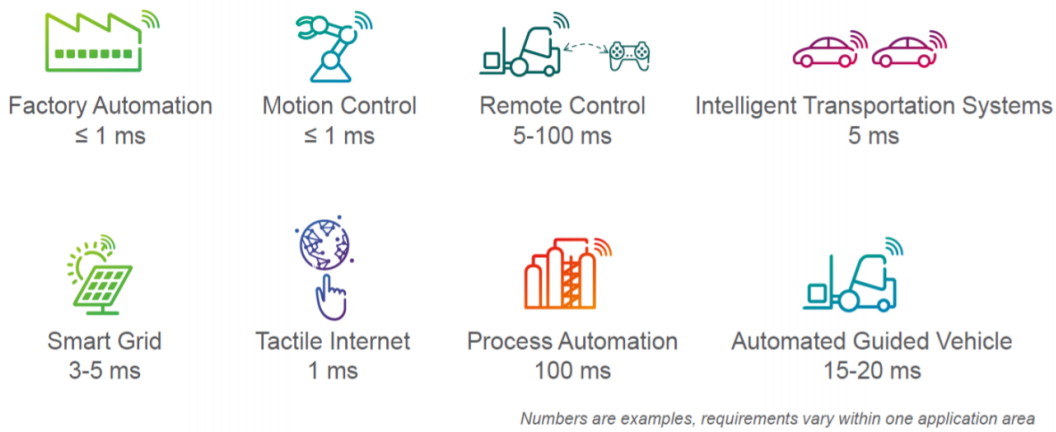

Figure 2 URLLC applications

- ***Tactile Internet***

  These use cases involve interaction between humans and systems, where humans wirelessly control real and virtual objects, and the interaction requires a tactile control signal with audio or visual feedback. Robotic controls and interaction include several scenarios with many applications in manufacturing, remote medical care, and autonomous cars. The tactile interaction requires real-time reactions on the order of a few milliseconds [5].

- ***E-health***

  E-health is a new healthcare approach with the support of information and communication technology. Remote Diagnosis, Emergency Response, Remote Surgery can be performed [3].

- ***Industrial automation***

  Industrial automation is a key application for URLLC features. Some industrial processes have extremely tight Key Performance Indicators (KPIs) for 5G communications links between sensors, actuators, and controllers. Examples use cases in this category include the following [5]:

  1. Motion control
  2. Industrial Ethernet
  3. Control-to-control communication
  4. Process automation
  5. Electric power generation and distribution

  Typical industrial automation use-cases requiring URLLC include factory, process, and power system automation. Use cases involve communication transfers enabling time-critical factory automation that are required in many industries across a wide spectrum that includes metals, semiconductors, pharmaceuticals, electrical assembly, food, and beverage.

- ***Intelligent transport system (ITS)***

  The realization of URLLC can empower several technological transformations in the transportation industry, including automated driving, road safety, and traffic efficiency services, etc. These transformations will get cars fully connected such that they can react to increasingly complex road situations by cooperating with others rather than relying on their local information.

  These trends will require information to be disseminated among vehicles reliably within an extremely short time duration. For example, in fully automated driving with no human intervention, vehicles can benefit from the information received from roadside infrastructure or other vehicles. The typical use cases of this application are automated overtake, cooperative collision avoidance, and high-density platooning, which require an end-to-end latency of 5 to 10milliseconds and a block error rate(BLER) down to 10^{-5} [5].

- ***Process automation***

  It is one of the crucial applications of URLLC which will not accept the latency of less than 1ms. It is largely used for industrial components and procedures which automates monitoring and decision system [3].

- ***Smart grid***

  Smart grid is an electrical grid that consists of several operational and energy modules, such as smart meters and devices, as well as renewable energy and energy-efficient resources [3].

- ***Augmented Reality (AR)***

  Augmented Reality (AR) and Virtual Reality (VR) bring higher bandwidth requirements in addition to URLLC constraints. The main difference between AR and VR is in the uplink requirements. VR needs low-data-rate pose estimates from the headset, while AR requires images of the view experienced by the user. It is a technique to augment the vision of the real-world environment by computer-generated information, such as audio, video, and geographic information [5].

2.3 Channel coding rate in the finite blocklength regime

For an AWGN channel with SNR i at a blocklength n and error probability ϵ, the achievable rate in bits per symbol can be closely approximated by [14],

$$R_i(\eta, \epsilon) \approx \log_2(1+\gamma_i) - \sqrt{\frac{V}{n}}\, Q^{-1}(\epsilon)\, \log_2 e \qquad (1)$$

Even though current coding and modulation schemes cannot yet fully achieve this rate, this model provides a much better description than a standard rate model.

For the lower values of SNR γ_i, the expression for $R_i\ (\eta, \epsilon)$ can become negative. Therefore, the achievable rate must be lower bounded by zero.

The researchers have assumed that there exist codes with blocklength n and error probability ϵ that achieve the rate $R_i^*(\eta, \epsilon)$ exactly. The throughput in time slot i is n. $R_i^*(\eta, \epsilon)$ bits if no transmission error occurs.

$$R_i^*(\eta, \epsilon) \approx max\ (R_i\ (\eta, \epsilon), 0) \qquad (2)$$

Determining $R_i^*(\eta, \epsilon)$, which describes the fundamental trade-off between rate, blocklength, and packet error probability in the transmission of information, is a fundamental problem in information theory. Shannon characterized the asymptotic behaviour of $R_i^*(\eta, \epsilon)$ in the limit n tends to infinity for general memoryless channels. Specifically, he showed that, for every $0< \epsilon <1$, the maximum coding rate $R_i^*(\eta, \epsilon)$ converges to channel capacity. The consequence of this result is that, for every transmission rate R less than C, there exists a sequence of coding schemes with rate R and vanishing packet error probability as n tends to infinity. Conversely, one can show that if $R_i^*(\eta, \epsilon)$, then the packet error probability over most memoryless channels of practical relevance (including the bi-AWGN channel goes to 1. This means that reliable communication is possible only at rates less than C, where C is $\log_2(1 + \gamma_i)$ [24].

It is worth stressing at this point that the channel capacity *C* is an asymptotic performance metric describing the behaviour of the maximum coding rate $R_i^*(\eta, \epsilon)$ in the limit $n \to \infty$. This means that capacity cannot be used to benchmark the performance of coding schemes in which the blocklength *n* is short, as it is expected in some 5G use cases, due, for example, to a latency constraint [24].

This observation has renewed the interest in non-asymptotic characterizations of the maximum coding rate $R_i^*(\eta, \epsilon)$. The exact computation of such a quantity is a formidable task unless the number *M* of codewords is very small. However, tight upper (converse) and lower (achievability) bounds on $R_i^*(\eta, \epsilon)$ that can be computed efficiently can be obtained for a variety of channels for practical interest for 5G using the finite-blocklength information-theoretic tools [24].

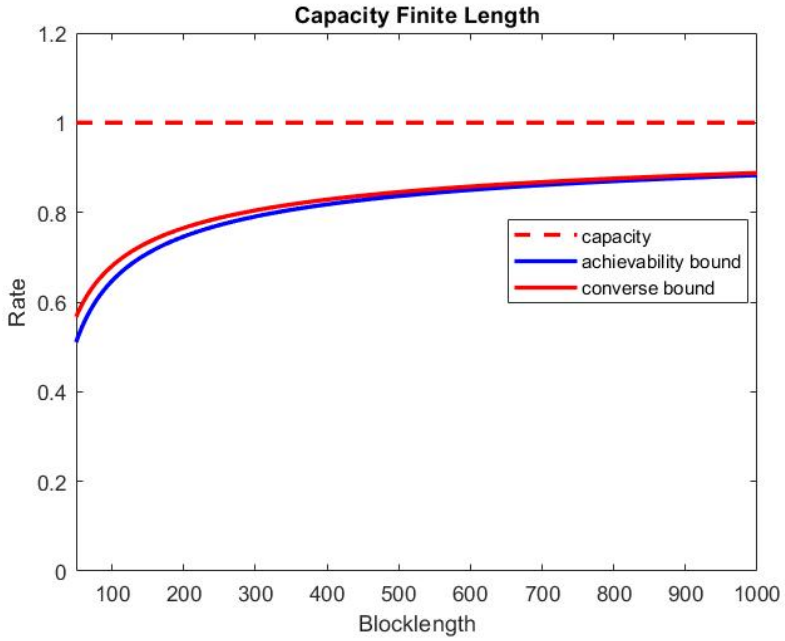

Figure 3 Capacity Finite Length

Such upper and lower bounds are depicted in figure 3 [14]. This illustrates the tightest known bounds as a function of the blocklength n, for a target error probability of 10^{-3} and SNR = 0dB. Equivalently, we can use the bounds to study the minimum packet error probability $R_i^*(\eta, \epsilon)$ achievable for a fixed blocklength n and rate R.

Relation between the Shannon (asymptotic) transmission rate and the actual transmission rate dependent on the block-length: Usually, the actual transmission rate is smaller than the asymptotic key generation rate. As the block-length increases, the actual transmission rate becomes closer to the asymptotic key generation rate.

2.4 Delay bound analysis

The design challenge for future applications is to allow wireless networks to operate extremely reliably at very short deadlines for rather small packets. A recently developed methodology provides probabilistic higher-layer delay bounds for fading channels when assuming transmission at the Shannon capacity limit. Based on this novel approach, the researchers have developed the service process characterizations for fading channels with finite blocklength channel coding, leading to novel probabilistic delay bounds that can give fundamental insight into the capabilities and limitations of wireless networks when facing low-latency M2M applications [6].

One of the biggest distinguishing factors between M2M and human-related applications is the requirements concerning the delay. For instance, in factory automation, there are often closed-loop control systems, where sensors, controllers, and actuators must exchange information with cycle times (i.e., delays) of 5 milliseconds and below while requiring reliability levels of $1 - 10^{-5}$ and higher (with respect to the deadline). Despite these tough requirements, packet sizes for these applications are typically rather small, i.e., only a few bytes need to be transmitted per datagram. Thus, the academic and

industrial research community faces the question how wireless networks can be designed to support such novel application types, also referred to as low-latency applications [6].

Many existing performance models assume that channel coding can provide error-free transmissions in a noisy channel and that those codes offer a data rate equal to the Shannon capacity. However, this model only holds in the limit of channel codes with infinite blocklength. In low-latency applications with small packet sizes and small block lengths, there is always a probability that transmissions fail due to noise. Furthermore, for high reliability, data must be encoded at a rate that is significantly lower than the Shannon capacity.

To characterize the possibilities and limitations of wireless networks for low-latency M2M applications, such finite-blocklength performance models need to be extended up to the application layer, where queueing effects are considered. One factor that causes queueing is channel fading, which means that the signal strength and thus the data rate of a wireless channel changes randomly over time. In general, it is difficult to analyse the queueing performance of fading channels due to the difficulty of finding a stochastic characterization of the random data rate. When the physical layer model also considers finite e block-length effects, the analysis at the application layer becomes even more challenging.

We consider data transmission between a data source, (e.g., a sensor in an industrial automation system) to another device (e.g., a control unit) over a wireless channel. A discrete-time model is used, i.e., time is divided into time slots with duration T. In each time slot i, the source generates a_i data bits and stores them in a queue. Then the queued data bits are transmitted over the wireless channel.

2.4.1 Queuing delay

The a_i data bits that are generated at the source correspond to the arrival process of the queueing system during time slot i. The departure process d_i describes the number of bits that arrive successfully at the destination. The departures depend both on the number of bits waiting in the queue and on the service offered by the wireless link. The service process s_i is equal to n. $R_i^*(\eta, \epsilon)$ when the transmission is successful, and a positive acknowledgment is received. When there is a transmission error, s_i has been set to zero. This means that the bits remain in the queue; they will be transmitted again in future time slots. Therefore, all data will eventually be transmitted to the destination and the queueing system is Lossless. The wireless link transmits the data from the queue in FIFO (First-in First-out) fashion [6].

The delay W(t) at time t describes the number of time slots it takes for information bit arriving at time t to be received at the destination. It is given as,

$$W(t) \triangleq inf\ \{u > 0 : A(0,t) \leq D(0,t+u)\} \qquad (3)$$

We are curious in finding a probabilistic bound on the delay W(t). Therefore, the target delay can be denoted as $\widehat{w}$. The probability that the delay is larger than $\widehat{w}$, i.e., that some data bits are not received within a certain deadline, is denoted by the delay violation probability $p_v(\widehat{w})$,

$$p_v(\widehat{w}) = \mathbb{P}\{W(t) > \widehat{w}\} \quad (4)$$

We assume that a system is reliable when only a very small percentage $p_v(\widehat{w})$ of bits is received after the deadline $\widehat{w}$. Our main goal in this work is to find an estimate for the delay violation probability $p_v(\widehat{w})$ when the rate of the channel code is given by the finite blocklength model. We propose a model that can be used to aid the design of communication systems that operates at low delay [6].

The reasons for not considering the Queuing are:

- If the inter-arrival time of the packet is longer than the duration of the packet, the packet exits from the buffer before the arrival of the next packet.
- If the packet duration is 1 second and the interarrival time of the packet is 0.1 second, it will automatically drop some of the packet due to the exceed in the capacity of the buffer.
- To make it simple, we already know that the size of the packet is small & the duration of the frame can be shorter when compared to the length of the UL transmission. Therefore, queuing can be neglected from the end-to-end delay.

Packet loss may result from factors other than transmission errors, such as queueing delay violation. Since some event-driven packets generated by different mobile users (MUs) arrive at a BS randomly, and the inter-arrival time between packets may be shorter than the transmission duration of each packet, there is a need to consider queueing delay. As a result, the overall packet loss not only comes from uplink (UL) and downlink (DL) transmission errors, but also from queueing delay violation. Because E2E delay and overall reliability are composed of multiple components, the queueing delay should be characterized by a delay bound and a delay bound violation probability for URLLC. Then tools for analysing average queueing delay cannot be used.

Two tools to analyse the queueing delay:

- Network Calculus
- Effective bandwidth

which are discussed in the below sub section.

2.4.1.1 Network calculus

One way to analyse the delay bound and delay violation probability is network calculus. The basic idea of network calculus is converting the accumulatively transmitted data and arrived data from the bit domain to the SNR domain. This is based on Stochastic network calculus allows the description and analysis of queueing systems through simple linear input-output relations. It comes under the type of Mellin transform [6].

Many of the input-output relationships of the queueing system can be expressed using these operators. The delay can be bounded as follows,

$$W(t) \leq inf\ \{u \geq 0: A \oslash S(t+u,t) \leq 1\} \quad (5)$$

which means that the delay violation probability $p_v(w) = \mathbb{P}\{W(t) > w\}$ can be bounded as,

$$p_v(w) \leq \mathbb{P}\{A \oslash S(t+w,t) > 1\} \quad (6)$$

This bound cannot be computed directly. However, it can be upper bounded again by using the Mellin transform [6]. Mellin Transform is a complex process. We have decided to proceed with the Effective bandwidth process.

Moreover, data requirement will be equal to the SNR requirement only when the bandwidth is given. Therefore, it is not suitable when bandwidth and transmits power are not defined. Moreover, even for power allocation, it is hard to obtain closed-form relation between transmit power and delay bound violation probability for unbounded arrival processes such as the Poisson process. As a result, it will be difficult to apply this tool to derive queueing delay constraints for resource allocation optimization.

2.4.1.2 Effective bandwidth

Different from network calculus, effective bandwidth can be used to design resource allocation in the bit domain. Effective bandwidth is the minimal constant service rate that is needed to serve a random arrival under a queueing delay requirement.

There are two key parameters taken into consideration. The first one is the time taken when we have certain bandwidth for the transmission and then the duration of the transmission.

For URLLC, the delay bound for each packet is usually less than 1 millisecond, which is shorter than the channel coherence time in typical scenarios. As such, the channel is constant within the delay bound, and the service rate is constant given a resource allocation policy. Therefore, the queueing delay requirement can be satisfied when the constant service rate equals the effective bandwidth. When only one packet is transmitted within a coding block, a constraint on D_q and ε_q for resource optimization can be imposed by setting the service rate required to transmit a packet. When the coherence time is shorter than the delay bound, effective capacity, a dual concept of effective bandwidth can be used together with effective bandwidth [7].

Since effective bandwidth is derived based on the large deviation principle, it is widely believed that it can only be used in the scenarios when the delay bound is large. Otherwise, the approximation on the queueing delay violation probability derived from the effective bandwidth is inaccurate. This can be applied for URLLC with burst arrival of traffic [7]**.**

2.4.2 Different cases in Delay

In this section, we will go through the different cases of delay such as end to end delay, packet loss probability, queueing delay violation and bit error rate.

2.4.2.1 End to end delay

E2E delay includes UL transmission delay, backhaul delay, queueing delay, and DL transmission delay. Packets go from AP to UAV directly without going through the central server. With fiber backhaul, backhaul delay is much shorter than 1millisecond, and hence will not be considered.

For the case in which the MUs are associated with a single BS, the transmission process is simpler and without backhaul delay. The transmission delay could be the duration of multiple frames, depending on the transmission policy, whether retransmission is allowed or not among subsequent frames. The control signalling also occupies some time/ frequency resources and leads to extra delay.

Typically, E2E delay < Interarrival time.

Typical E2E delay in URLLC is shorter than the inter-arrival time between packets in machine-type communications and the CNPC links of the UAVs. Therefore, we consider that there is no queueing at the UAVs. It follows that a packet is either transmitted successfully or discarded due to delay violation before the arrival of the next packet.

Whereas in LTE systems, TTI is 1millisecond, and a frame consists of 10 TTIs. As a result, the transmission delay far exceeds the required E2E delay for URLLC. To reduce transmission delay, a short frame structure is used whose duration equals one TTI, and each frame includes a phase for control signalling except the phases for UL and DL data transmissions. With short blocklength channel codes, coding delay does not exceed transmission duration, and hence does not need to be considered [2].

2.4.2.2 Packet loss probability

We consider that a packet is lost when either UL or DL transmission fails, and the overall packet loss probability should not exceed $\varepsilon_{\max}$ to satisfy the reliability requirement in URLLC. Hence, the packet loss probabilities in UL and DL transmissions are set to be equal. i.e., the UL and DL packet loss probabilities should not exceed,

$$\varepsilon_{max}^{u} = \varepsilon_{max}^{d} = \varepsilon_{max} / 2 \qquad (7)$$

since it is near optimal in terms of minimizing the required total bandwidth. As such, the requirement on the overall packet loss probability can be decoupled into two requirements on UL and DL packet loss probabilities, respectively [2].

2.4.2.3 Queueing delay violation

When serving randomly arrived packets with a wireless link, it is difficult to guarantee a delay bound with probability one. To optimize resource allocation with the constraint on queueing delay bound and queueing delay translate the queueing delay requirement into the constraint on resource optimization.

In typical application scenarios of URLLC, the required delay is shorter than the channel coherence time. To ensure the queueing delay requirement (and transmission error probabilities), the transmit power may become unbounded in fading channels. To satisfy the queueing delay requirement with finite transmit power, when a channel is in deep fading, some packets that cannot be transmitted even with the maximal transmit power can be discarded proactively. Hence, the third component is from the proactive packet dropping [7].

2.4.2.4 Bit error rate (BER)

The bit error rate required to achieve reliability is based on how correlated the decoded bit errors are, which depends on the error correction scheme. An interleaver is usually combined with AWGN channel codes to correct for long error bursts which may occur in deep fading or due to burst interferences [3].

In URLLC scenarios, the size of the block length is typically too short to effectively ensure reliable communications. Therefore, Shannon's capacity is no longer applicable, and the decoding error probability cannot be arbitrarily small. The obtainable capacity when transmitting shorter blocks and the design of short codes for small block size has been increasingly attracting attention.

Over a single link (e.g., just UL), if the decoded bit errors are uncorrelated, the required decoded BER, referred to as the information BER (IBER), is related to the BLER and reliability as [3],

$$\text{Reliability} = 1 - \text{BLER} = (1 - \text{IBER})^{*}8X \qquad (8)$$

When transmitting X bytes in time t_i and bandwidth B_i, the required coding rate is $R_i = 8X/B_i t_i$ (in bits per channel use).

Let $\text{IBER}_i(t_i,X)$ and $\text{BLER}_i(t_i,X)$ respectively be the IBER and BLER on the link i in a quasi-static fading channel. From finite blocklength information theory, in typical URLLC transmissions with finite blocklength M,

$$\text{BLERi}\ (\text{ti},X) \approx E\left[Q\left(\sqrt{\left(\frac{M}{V(\gamma_i)}\right)}\left(\gamma_i C(\gamma_i) - R_i\right)\right]\right. \qquad (9)$$

where,

γ_i - random variable
SINR - received signal to interference-plus-noise ratio
$\varepsilon_i(\gamma_i)$ - BLER under a given received SINR γ_i on link i
E[.] - expectation function

$$C(\gamma) = log_2(1+\gamma) \tag{10}$$

$$Q(w) = \int_w^\infty {}^1\!/_{\sqrt{2\pi}}\ e^{-\frac{t^2}{2}}\, dt \tag{11}$$

$$V(\gamma) = \frac{\gamma(\gamma+2)}{(1+\gamma)^2\ log_2^2\, e} \tag{12}$$

It is reasonable to assume that the received SINR γ_i is static during one URLLC transmission since the transmission time can be shorter than the coherence time of the channel.

3 UAV-based communication: application and modelling

With their high mobility and low-cost UAVs, commonly known also as drones or remotely piloted aircraft, have found a wide range of applications during the past few decades. UAV-enabled solutions, systems, and networks are considered for various applications ranging from military and security operations to entertainment and telecommunications commercial, agriculture, scientific research, cargo, and other piloted and passenger-carrying aircraft.

UAVs can be used as complementary infrastructure to provide wireless services for the ground users or they may require wireless connectivity from the ground for a safe and reliable operation. For these, indeed, an adequate UAV integration into ground wireless networks is required.

When UAVs are used as flying aerial base stations, they can support the connectivity of existing terrestrial wireless networks such as cellular and broadband networks. Compared to conventional, terrestrial base stations, the advantage of using UAVs as flying base stations is their ability to adjust their altitude, avoid obstacles, and enhance the likelihood of establishing LoS communication links to ground users.

In this chapter, I have discussed the classification of UAVs, architecture and challenging aspects, applications and regulations of UAVs.

3.1 Classifications of UAV

UAVs can be broadly classified into two categories:

- ***Fixed wing***

Fixed-wing UAVs usually have high speed and heavy payload, but they must maintain continuous forward motion to remain aloft, and thus are not suitable for stationary applications like a close inspection [9].

- ***Rotary-wing***

In contrast, rotary-wing UAVs such as quadcopters, while having limited mobility and payload, can move in any direction as well as stay stationary in the air [9].

The choice of between one of the two above UAVs depends on the application and goals. One needs to use an appropriate type of UAV that can meet various requirements imposed by the desired QoS, the nature of the environment, and federal regulations. It is worth noting that the flight time of a UAV depends on several factors such as energy source (e.g., battery, fuel, etc.,), type, weight, speed, and trajectory of the UAV [8].

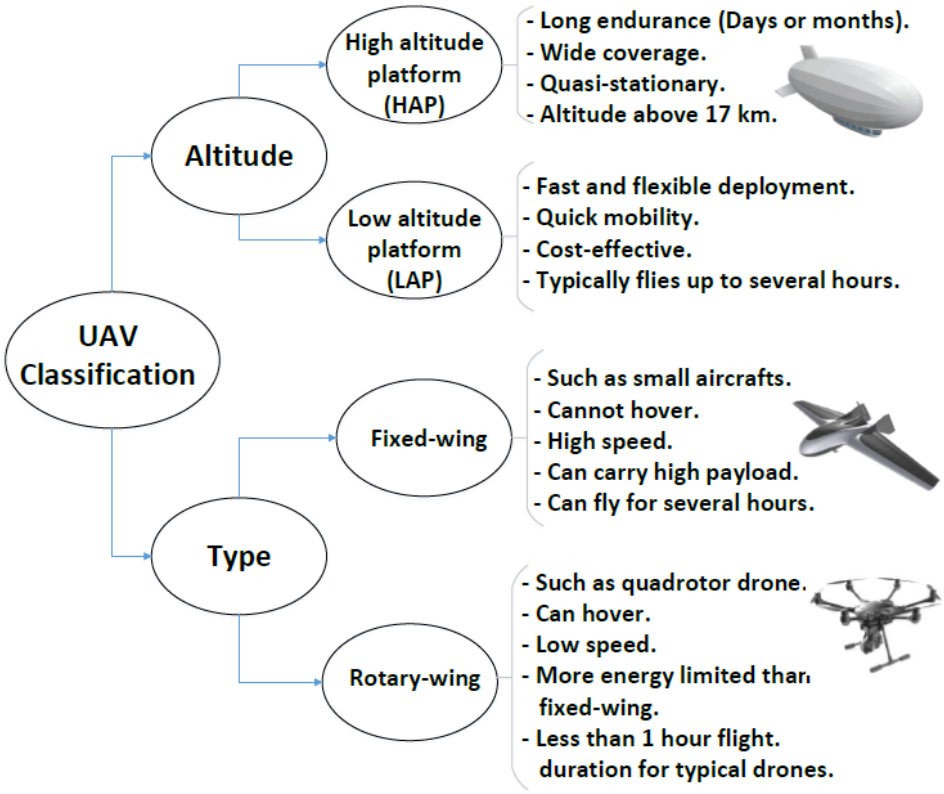

Figure 4 UAV Classification

UAV can be further categorized based on their altitudes as shown in figure 4 [8] :

To properly use UAVs for any specific wireless networking application, several factors such as the UAVs' capabilities and their flying altitudes must be considered.

- ***High altitude platforms (HAPs)***

HAPs have altitudes above 10,000 metres and are typically quasi-stationary, which usually operate in the stratosphere that is tens of kilometres above the Earth's surface [9].

- ***Low altitude platforms (LAPs)***

LAP can fly at altitudes of tens of meters up to a few kilometres lies below stratosphere, can quickly move, and are flexible [9].

Low altitude platforms are quasi-stationary aerial platforms such as quadcopters, balloons, and helicopters, usually characterized with an altitude laying within the troposphere. Contrary to LAP, High Altitude Platforms (HAP) that can reach the upper layers of the stratosphere. In general, LAP is much easier to deploy and are in line with the broadband cellular concept since low altitude combines both coverage superiority and confined cell radius. The technology carried by LAPs depends on the end user's application, budget, and bandwidth requirements [10].

According to US Federal aviation regulations, the maximum allowable altitude of LAP that can fly freely without any permit is 400 meters. Compared to HAPs, the deployment of LAPs can be done more rapidly thus making them more appropriate for time-sensitive applications.

Moreover, LAPs can be readily recharged or replaced if needed. In contrast, HAPs have longer endurance and they are designed for long-term (e.g., Can be in the air for up to a few months) operations. Furthermore, HAP systems are typically preferred for providing and wide-scale wireless coverage for large geographic areas. However, HAPs are expensive, and their deployment time is significantly longer than LAPs.

3.2 UAV architecture overview

Although 3GPP is still concentrating its efforts on cellular-connected UAVs standardization, different proposed wireless architectures involve flying systems carrying an intelligent router. The architecture involving aerial base station is generally characterized by two basic types of communication links [9]:

- Control and non-payload communications link
- Data link

which are discussed in the following sections.

3.2.1 Control and non-payload communications link (CNPC)

The CNPC links are essential to ensure the safe operation of UAV systems. Highly reliable, low-latency, and secure two-way communications, usually with low data rate requirements, must be supported by these links for exchanging safety-critical information among UAVs, as well as between the UAV and ground control stations (GCS), such as dedicated mobile terminals mounted on ground vehicles.

The main CNPC information flow can be broadly categorized into three types [9]:

- Command and control from GCS to UAVs
- Aircraft status report from UAVs to ground
- Sense-and-avoid (Collision avoidance) information among UAVs.

The CNPC link is also used for delivering information about the network configuration, which determines the time and frequency resource allocation, and to collect some information about the UAV flight data (such as GPS, relative elevation angle, and flight speed), residual energy, and performances about the provided connectivity (such as average bit error rate, received and transmitted power).

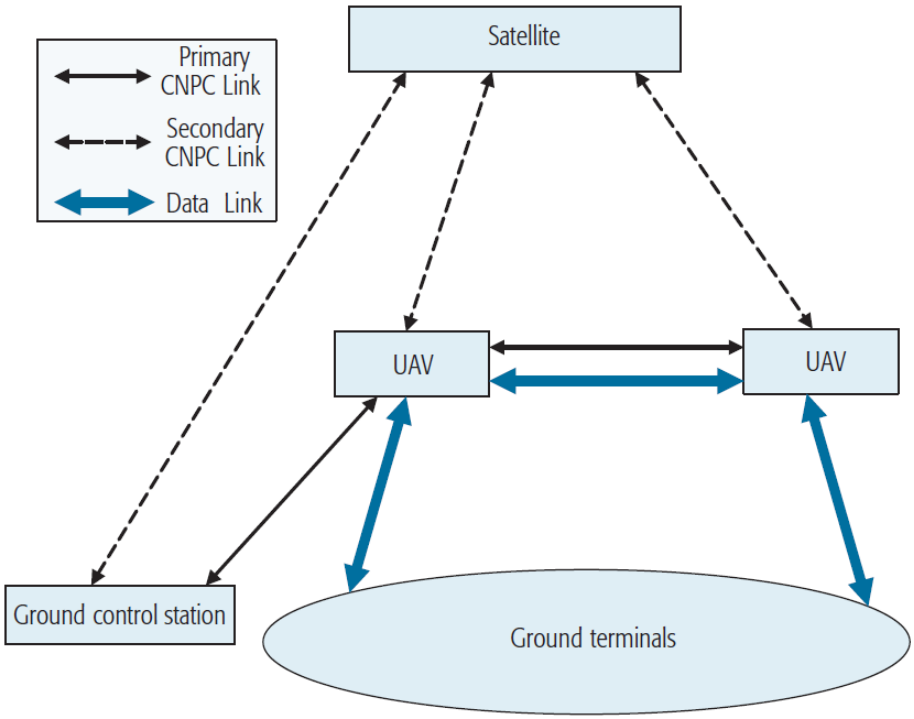

Figure 5 Basic networking architecture of UAV

Figure 5 shows the basic networking architecture of UAV-aided wireless communication [9].

Even for autonomous UAVs, which can accomplish missions relying on onboard computers without real-time human control, CNPC links are also necessary in case emergency human intervention is needed. Air traffic control (ATC) links, which are necessary only when the UAVs are within controlled airspace (e.g., near an airport) [11].

3.2.1.1 Spectrum for CNPC

Due to the critical functions to be supported, CNPC links should in general operate in a protected spectrum. Currently, two such bands have been allocated: The L-band (960–977 MHz) and the C-band (5030–5091 MHz). Furthermore, although the direct links between GCS and UAVs (primary CNPC links) are always preferred for delay reasons, secondary CNPC links via satellite could also be exploited as a backup to enhance reliability and robustness [9]. Another key requirement for CNPC links is a superior security .

Effective security mechanisms should be employed to avoid ***a ghost control*** scenario, a potentially catastrophic situation in which the UAVs are controlled by unauthorized agents via spoofed control or navigation signals. Therefore, powerful authentication techniques, possibly complemented by the emerging physical layer security techniques, should be applied for CNPC links [9].

3.2.2 Data link

The data links, on the other hand, aim to support mission-related communications for the ground terminals, which, depending on the application scenarios, may include terrestrial base stations (BSs), mobile terminals, gateway nodes, wireless sensors, and so on. Taking the UAV-aided ubiquitous coverage shown in Fig 4. as an example, the data links maintained by the UAVs need to support the following communication modes [9]:

- Direct mobile-UAV communication as for BS offloading or during complete BS malfunction.
- UAV-BS and UAV-gateway wireless backhaul.
- UAV-UAV wireless backhaul.

The capacity requirement for these data links ranges from several kilobits per second in UAV-sensor links to dozens of gigabits per second in UAV-gateway wireless backhaul. Compared to CNPC links, the data links usually have higher tolerance in terms of latency and security requirements. In terms of spectrum, the UAV data links could reuse the existing band that has been assigned for the applications to be supported, (e.g., the LTE band while assisting cellular coverage), or a dedicated new spectrum could be allocated for enhanced performance (e.g., using millimeter-wave (mmWave), band for high-capacity UAV-UAV wireless backhaul). In summary, a payload communication typically requires a high data rate with relaxed latency requirements up to several hundreds of milliseconds.

3.2.3 Current Technologies for UAV Communication

The existing technologies for UAV communication consist of [12]:

- ***Direct Link to Ground Station***

  This technology is for connecting the UAV to a ground station over an unlicensed spectrum such as the Industrial Scientific Medical (ISM) 2.4 GHz band. This method is basically for establishing an LoS connection that notably limits the range of UAV's operation. Particularly, in an urban environment, where there are several types of blockages of high heights, the communication link is likely to be discontinued. Therefore, such links cannot be reliable and safe. Furthermore, an unlicensed spectrum is typically insecure and vulnerable to interference and jamming.

- ***Satellite***

  Satellite-assisted communication provides global coverage even in remote areas or over oceans where there is no existing ground infrastructure. Satellites can assist to navigate and localize UAVs. Besides, the communication with the ground stations or between UAVs can be set via satellite relay. However, the communication delay to satellite is typically very high and not suitable for CNPC. Moreover, the link length is large and channel LoS is significant. Therefore, establishing a reliable link is questionable. Finally, the cost of using satellites restricts such technology to be used for dense UAV deployments.

- ***Flying Ad-Hoc Network (FANET)***
  UAVs can leverage the current technology in building up a mobile ad-hoc network using for instance IEEE 802.11 a/b/g/n. Such networking is typically independent of the ground infrastructure and enables self-organized peer-to-peer communication. In this case, UAVs can act as a relay to forward data to connect far away UAVs. However, such a method imposes a long end-to-end delay and is not spectrum efficient. Moreover, connecting massive UAVs via a reliable routing protocol is very complex and difficult to manage.

3.2.4 UAV Information Dissemination

Thanks to their mobility and LoS opportunity, UAVs can assist the ground-based networks by information dissemination. Due to interference issues or limited battery capacity, the ground transmitters may lower their transmit power (e.g., IoT devices) or establish a communication link only in short distances (e.g., D2D case). In such a situation a rapid deployment of UAVs can assist to broadcast common files. For instance, UAVs can increase the reliability of upcoming autonomous vehicular technology by broadcasting safety information. Also, in an emergency, a UAV can act in a D2D mode and spread critical information to the ground nodes promptly [12].

3.2.5 Data Collection in UAV

UAVs can be deployed to collect data produced by low-power IoT devices or wireless sensors distributed over a certain region. Such data might be delay-tolerant information and hence does not need an instant connection to the central unit using the permanent expensive ground infrastructure. Nevertheless, real-time communication can also be facilitated by using UAV relays between IoT nodes and the BSs. In effect, UAVs can fly above the ground nodes and establish an LoS connection with both the ground nodes and the target BSs. Therefore, the communication links turn to be more reliable, and the coverage range is potentially extended. In this manner, UAVs can address several challenges in IoT-centric scenarios [12].

3.2.6 Placement considerations

The problem of finding an optimum location or path planning is more challenging for UAVs compared to the conventional terrestrial BSs. On one hand, UAVs can freely move in space without any borders whereas there are also a variety of applied constraints that need to be considered, e.g., maintain LoS connectivity, energy limitation, and obstacles collision avoidance, many of which are time-dependent and are difficult to predict.

In most cases, the optimal solution is application-based. For instance, in the case of cellular coverage UAVs supported, the solution is to deploy static UAVs that hover above the centre of the area to be covered. In the case of real-time applications or

moving devices, it is more intuitive to employ more than one UAV to cooperatively achieve low delay and high-reliability communications. Also, in the case of energy-aware deployment, several UAVs need to cooperate letting the UAVs leave the serving area for energy replenishment, meanwhile the connectivity gap is filled by neighbouring UAVs, for example, via increasing the transmission power or adjusting the aircraft position [13].

3.2.7 Key and challenging aspects

The integration of UAVs into wireless cellular networks as aerial communication platforms brings new network infrastructure design possibilities and challenging aspects to consider. Indeed, there are many differences compared to the terrestrial counterpart [13].

- ***High altitude:***

The typical height of terrestrial BSs is around 10-20 meters in a urban scenario, whereas the current regulation allows the ABSs to hover up to 100-120 meters. This enables the ABS to achieve broader coverage compared to classical terrestrial infrastructure and reduce the interference from other terminals. The ground terminals can be easily discernible at different altitudes and elevation angles measured concerning UAVs.

- ***3D high mobility and user tracking:***

UAV can provide a higher line of sight (LoS) channel probability than classical ground-to-ground communications that generally suffer more path LoS attenuation and fading effects. Transceivers can track the moving users (pedestrian, connected vehicles or Internet of things devices) maintaining a stable LoS connection.

- ***Energy-efficient design:***

In general, UAVs are energy-limited systems. This aspect poses critical bounds on their hovering and flight time, and some trade-offs can arise in terms of quality of services provided to a user (i.e., transmitted power) and energy constraints.

- ***Security and surrounding environment health*:**

UAVs need to be continually monitored to avoid incidents and maintain safety distance with other aerial vehicles, buildings, and obstacles. For this purpose, a control link is established with the terrestrial backhaul network.

- ***Privacy and data protection:***

The information collected by the onboard sensors is an issue in terms of both individual's and business privacy.

3.2.8 Impact and applications scenarios

UAVs allow a mobile operator/connectivity provider or network designers to create on-demand networks in a bordered area that cater to clients and use cases. Lightweight, Commercial BSs are suitable to be mounted on UAVs with a moderate payload allowing a wide range of applications [13].

- Effectively accompaniment existing terrestrial systems in crowded areas (e.g., stadium during a sports event or live performances) by providing additional capacity.
- Information dissemination and collection in wireless sensor networks and IoT scenarios (smart city or in fields for terrain inspection and precision agriculture) where, due to low transmitted power of the devices, long-range communications are not possible.
- Information transmission among geographically separated data centers or delivering network coverage in hard-to-reach rural or suburban areas, where deploying ABSs becomes highly advantageous compared to expensive telecommunications towers for BS or fiber links installation.
- Fast connectivity restoration after infrastructure failure or data relaying in emergency situations such as terroristic attacks. An example is a link between the frontline and the headquarters during such unpredictable situations.

3.2.9 UAV Regulations

Regulatory issues are important limiting factors facing the deployment of UAV-based communication systems. Despite the promising applications of UAVs in wireless networks, there are several concerns regarding privacy, public safety, security, collision avoidance, and data protection. In this regard, UAV regulations are being continuously developed to control the operations of UAVs while considering various factors such as UAV type, spectrum, altitude, and speed of UAVs [13].

In general, five main criteria are often considered when developing UAV regulations,

1) Applicability:

Pertains to determining the scope (considering type, weight, and role of UAVs) where UAV regulations are applied.

2) Operational limitations:

Related to restrictions on the locations of UAVs.

3) Administrative procedures:

Specific legal procedures could be needed to operate a UAV.

4) Technical requirements:

It includes communications, control, and mechanical capabilities of drones.

5) Implementation of ethical constraints:

Related to privacy protection.

UAV regulations vary between different countries and types of geographical areas (e.g., Suburban, urban). In the United States, regulations for UAV operations are issued by the Federal Aviation Authority (FAA) and National Aeronautics and Space Administration (NASA). NASA is planning to develop UAV control frameworks in collaboration with Federal Communications Commission (FCC) and FAA. FCC is currently investigating if a new spectrum policy needs to be established for drone operations [13].

3.3 Fundamentals of Air-to-Ground channel modelling

At first, let us have an overview of the classical wireless channel model, fundamental characteristics of the ground-UAV channel and modelling the line-of-sight probability.

3.3.1 Classical wireless channel model

The wireless link is modelled as a single-antenna Rayleigh fading channel, where the SNR γ_i at the receiver varies over time. Assume a block-fading model where the SNR remains constant during each time slot and varies independently from one-time slot to the other SNR values in different time slots are independent and identically distributed (i.i.d.) with exponential distribution.

$$F(\gamma_i) = \frac{1}{\bar{\gamma}}\, e^{-\frac{\gamma_i}{\bar{\gamma}}} \tag{13}$$

$\bar{\gamma}$ - average SNR at the receiver

Transmits N symbols, which consist of n symbols for data transmission and n_h symbols for feedback and acknowledgments from the receiver. The system thus occupies a bandwidth of N/T [Hz].

In each time slot i, the transmitter uses a channel code of length n and rate R_i to encode the first nR_i bits in the queue and then transmits the codeword to the receiver. The receiver replies with an acknowledgment, which is assumed to be instantaneous and error-free. Furthermore, it has been assumed that the transmitter has perfect estimates of the instantaneous SNR and adapts the coding rate R_i according to i. A standard rate model that is often applied in wireless networking research, assumes that the achievable rate R_i in bits per (complex-valued) symbol is equal to the Shannon capacity of the channel, and no errors occur.

The Shannon capacity is an upper bound for codes which only holds when the blocklength n tends to infinity. At finite blocklength, there is always a probability $\epsilon > 0$ that a transmission error occurs. This error probability can be reduced by decreasing the rate of the code.

3.3.2 Air-to-Ground path LoS modelling

Wireless signal propagation between the transmitter and the receiver is affected by the medium. ATG Channel characteristics for UAV to ground transmission differs from the classical ground communication channel characteristic. Due to the different propagation environment and elevation angle between the Tx and Rx in ATG,ATG links experience lower path LoS and shadowing compared to the classical cellular networks.

To clarify this fact, let us consider a given ground terminal and a UAV at altitude with a ground distance 2D of r. Accordingly, the UAV is seen by the elevation angle of $\theta = \tan^{-1}(h/r)$ from the ground terminal as illustrated in figure 6 [12]. We consider two extreme cases for the ground terminal that aims to communicate with the UAV in an urban environment [12]:

1. $\theta \rightarrow 0$: In this case, which is equivalent to $h \rightarrow 0$ (for $r \neq 0$), the channel behaviour follows ground to ground models where the presence of many obstacles results in a dramatic drop of the received power. This significant power decay can be reflected onto the channel model by proposing a large pathloss exponent α and severe shadowing and small-scale fading effects. For this case the channel between a transmitter and receiver is roughly always NLoS as the probability of LoS converges to zero.

2. $\theta \rightarrow 90$: In this case, which is equivalent to $h \rightarrow \infty$ (for $r \neq 0$), the probability of LoS PLoS converges to one and the channel adopts roughly free space characteristics. Accordingly, a lower pathloss exponent and a lighter small-scale fading and shadowing effects are experienced since the environment between the transmitter and receiver becomes less obstructed.

The above-mentioned intuition encourages to model the drone communication channel depending on the elevation angle (or equivalently altitude) as this, easily observable variable, presents a strong correlation with the link quality.

With this, we studied a statistical propagation model by considering two major groups of received power and their probability of occurrence, namely LoS and dominant NLoS components but still receiving coverage via strong reflections and diffractions. This model captures different urban environment properties and proposes a θ dependent pathloss and shadowing prediction of the communication channel between a terrestrial and an aerial node.

For the shadowing effect where a log-normal distribution is considered separately for each LoS and NLoS component. The standard deviation of each group $\sigma LoS(\theta)$ and $\sigma NLoS(\theta)$ is characterized using a negative exponential dependency with the elevation angle in which a lower elevation angle and hence altitude leads to a larger variation around the average pathloss. The overall average shadowing effect in the links can be represented by the standard deviation written as

$$\sigma^2(\theta) = P_{LOS}^2(\theta).\sigma_{LOS}^2(\theta) + [1 - P_{LOS}(\theta)]^2.\sigma_{NLOS}^2(\theta) \quad (14)$$

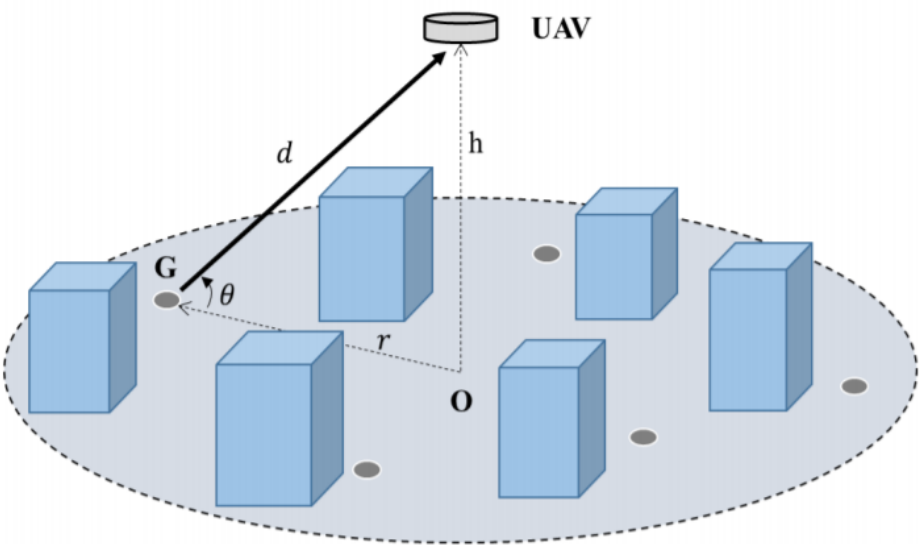

Figure 6 Illustration of a ground-UAV link in an urban area

As the drone goes higher the fluctuation due to shadowing gradually diminishes owing to the presence of fewer obstacles between the transmitter and receiver [12].

In addition to the shadowing and scattering caused by the man-made structures, it also introduces additional pathloss in the ATG link. We refer to the additive pathloss incurred on top of the free space pathloss as the excessive pathloss, which has a Gaussian distribution. Mean value (expectation) rather than with its random behaviour, hence η here refers to the mean value of the excessive pathloss. Another point is that the effect of small-scale fluctuations caused by the rapid changes in the propagation environment is not considered.

Accordingly, the resulting ATG mean pathloss (expressed in dB) can be modelled as:

$$PL_{\xi} = FSPL + \eta_{\xi} \tag{15}$$

where FSPL represents the free space pathloss and ξ refers to the propagation group. Noticing that, the excessive pathloss η affecting the ATG link depends largely on the propagation group rather than the elevation angle which is depicted θ [10].

P(ξ*;* η) represents the probability of occurrence of a certain propagation group that is strongly dependent on the elevation angle. We follow the assumption of the two dominant propagation groups that strictly correspond to the LoS condition. Accordingly, $\xi \epsilon$ {LoS*;* NLoS}, and the groups' probability are linked as the following:

$$P(NLOS, \theta) = 1 - P(LOS, \theta) \tag{16}$$

The probability of LOS increases with an increase in altitude and in elevation angle [10].

3.3.3 Modelling the line-of-sight probability

The pathloss between the UAV and the ground node depends on the locations of the UAV and the ground node as well as the type of propagation environment (e.g., Suburban, urban, dense urban and high-rise urban). Depending on the environment, ATG communication links can be either LoS or NLoS. Note that, without any additional information about the exact locations, heights, and the number of the obstacles, one must consider the randomness associated with the LoS and NLoS links. The probability of occurrence is a function of environment, density and height of buildings, and elevation angle between the UAV and ground node [16].

To cover a wide range of possible applications for this model, four simulation environments were selected,

(i) Suburban Environment that also covers the rural areas.
(ii) Urban Environment which is the most common situation representing average European cities.
(iii) Dense Urban Environment representing some types of cities where buildings are in proximity with each other.
(iv) High-rise Urban Environment with tall buildings, representing modern cities with skyscrapers style.

The International Telecommunication Union (ITU) in its recommendation document suggests a remarkable method for finding the probability of geometrical LoS between a terrestrial transmitter at elevation h_{TX} and a receiver at elevation h_{RX} in an urban environment. This probability is dependent on three statistical parameters related to the urban environment [16]:

Parameter α: Represents the ratio of built-up land area to the total land area (dimensionless).

Parameter β: Represents the mean number of buildings per unit area (buildings/km2).

Parameter γ: A scale parameter that describes the building's heights distribution according to Rayleigh probability density function. Clearly, due to the randomness (uncertainty) associated with the height of buildings (from a UAV perspective), one needs to consider a probabilistic LoS model while designing the UAV-based communication systems.

$$F(H) = \frac{H}{\gamma^2}\, exp^{-\frac{H^2}{2\gamma^2}} \tag{17}$$

H is the building height in meters.

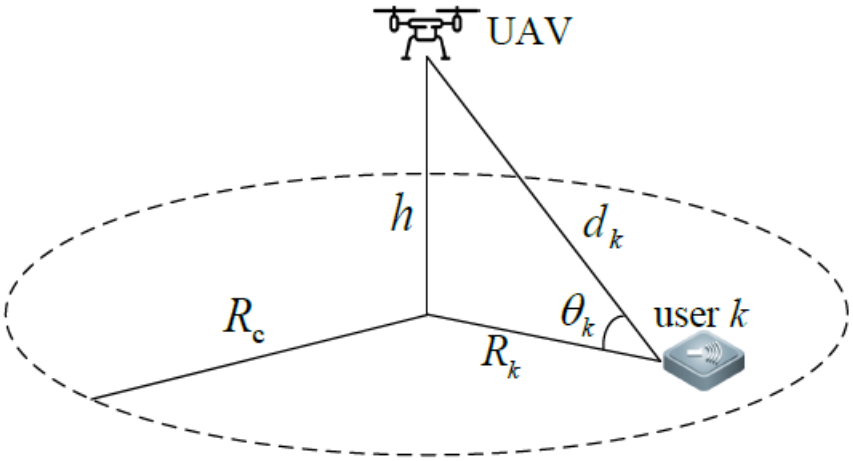

Figure 7 Ground-to-air channel model [1]

After some mathematical calculations, the resulting LoS probability can be written as,

$$P(LOS) = \prod_{n=1}^{m}\left[1 - \exp\left(-\frac{\left[h_{TX} - \frac{\left[\left(n+\frac{1}{2}\right)(h_{TX}-h_{RX})\right]^2}{m+1}\right]}{2\gamma^2}\right)\right] \quad (18)$$

where m = floor $(r\sqrt{(\alpha\beta)} - 1)$ and r is the ground distance between the transmitter and the receiver, while n is merely the product index. It is worthy to mention that the geometrical LoS is independent of the system frequency, also that equation 18 is generic and can be used for any h_{TX} and h_{RX} heights. In the case of a UAV, we can disregard h_{RX} since it is much lower than the average building's heights and the UAV altitude [10].

Also, the ground distance becomes $r = h / \tan(\theta)$. It is important to note that the resulting plot of the series in the above equation, will smooth out for large values of h, accordingly PLoS can be considered as a continuous function of θ and the environment parameters as shown in figure 7 [1]. We can notice that the trend can be closely approximated to a simple modified Sigmoid function (S-curve) of the following form [16]:

$$P(LOS, \theta) = \frac{1}{1+\emptyset \exp(-\psi\,[\theta_k - \emptyset])} \quad (19)$$

where $\emptyset$ and ψ are called here the S-curve parameters.

$\emptyset$ and ψ are constants that depend on the types of communication environments (e.g., suburban, urban, dense urban, and high-rise urban).
θ_k is the elevation angle.
h is the altitude of the UAV.
R_k is the distance from the user to the projection of the UAV on the ground.

This approximation significantly eases the calculation of the LoS probability. It is observed that the LoS probability increases with the elevation angle, which is reasonable as the probability that the signal is blocked is decreasing when the height of the UAV is increasing.

To generalize the solution, the researchers have linked the S-curve parameters $\emptyset$ and ψ directly to the environment variables α, β and γ [16]. This linking was performed using two variables surface fitting where (α*β) is assumed as the first variable, and (γ) as the second. The surface equation 20 yields a two-variables polynomial having the following form:

$$Z = \sum_{j=0}^{3} \sum_{i=0}^{3-j} C_{ij} \alpha \beta^{i} \gamma^{j} \quad (20)$$

where Z represents the fitting parameter $\emptyset$ or ψ, and C_{ij} are the polynomial coefficients [16].

3.3.4 Surface fitting environmental variables

The surface equation yields a two-variables polynomial and C_{ij} is the precalculated polynomial coefficients given in tables 1 and 2 below and their respective simulation results are shown in figures 8 and 9.

Table 1 Surface polynomial coefficients for a

C_{ij}	i	0	1	2	3
j					
0		9.34E-01	2.30E-01	-2.25E-03	1.86E-0.5
1		1.97E-02	2.44E-03	6.58E-06	-
2		-1.24E-04	-3.34E-06	-	-
3		2.73E-07	-	-	-

Table 2 Surface polynomial coefficients for b

C_{ij}	i	0	1	2	3
j					
0		1.17E+00	-7.56E-02	1.98E-03	-1.78E-05
1		-5.79E-03	1.81E-04	-1.65E-06	-
2		1.73E-05	-2.02E-07	-	-
3		-2.00E-08	-	-	-

Figures below has been plotted for the S-curve parameters 3D-fitting Phi and Psi as a relation to the high-urban environment.

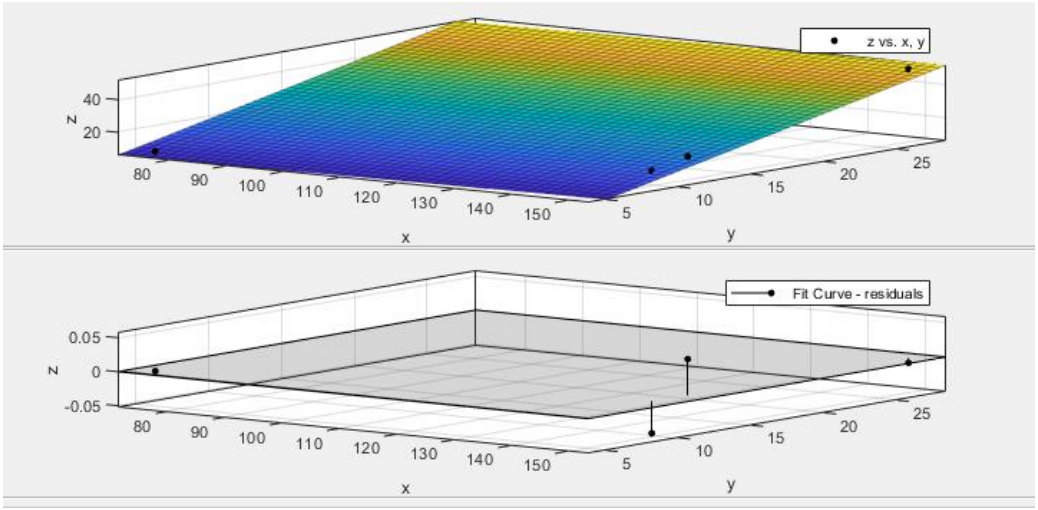

Figure 8 3D-Fitting Curve - Phi

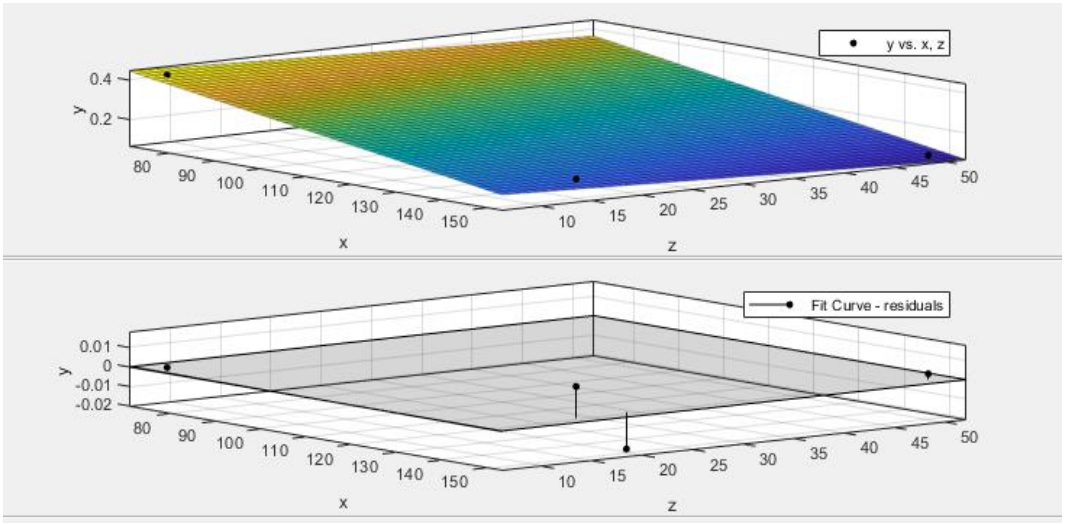

Figure 9 3D-Fitting Curve - Psi

Thus, we have gone through the background and key concepts of UAV and the classical wireless channel.

4 Single UAV-Assisted Uplink Transmission

To enable URLLC in the control and non-payload communication of the UAV, we need to reduce the latency and increase the reliability. We need to find out the maximum available range between the UAV and the GCS. Multi-antenna GCS consists of multiple distributed Access Points (APs) that exchanges latency-critical control information with multiple UAVs via short packets.

The available range is the maximum horizontal distance in which the round-trip delay and overall packet loss probability can be achieved with a required probability. The characterization of the available range bears in mind the decoding error probability in the short block length and the correlation of links from the APs to UAV. The available range can be maximized by optimizing the altitude of UAVs, the duration of the uplink and downlink phases, and the antenna configuration. GCS contains many APs, and each AP can have multiple numbers of antennas.

A typical local communication scenario for URLLC where each MU is served by one of the adjacent BSs, which are linked by a single hop backhaul. When packets are generated at an MU, it first uploads the packets to its BS. The BS then forwards these packets to the other BSs with which the target MUs are associated. Finally, the BSs send packets from their buffers to the target MUs.

In our scenario, we consider the K single antenna UAVs communicating with ground control station which are operating at the same altitude h. We define the minimum and the maximum range altitude of UAV as h_{min} and h_{max} accordingly. Therefore, the range of h lies in between $h_{min} \leq h \leq h_{max}$.

To satisfy reliability and latency requirements, strong interference should be avoided. Therefore, users in adjacent cells use different bandwidths as shown in figure 10 and the inter-cell interference can be considered as noise. Orthogonal frequency division multiple access is used to avoid interference among users in each cell [1].

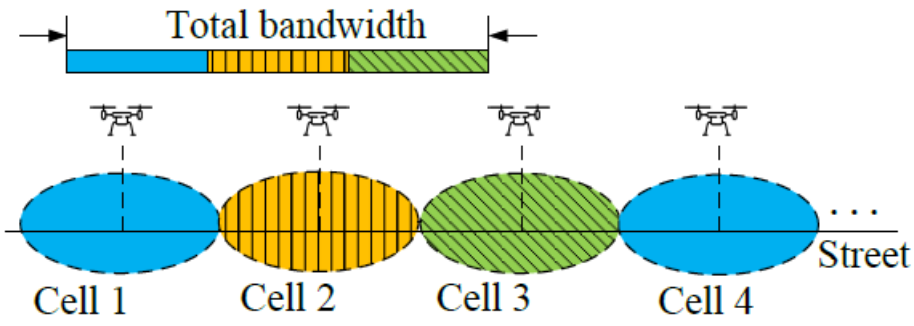

Figure 10 Bandwidth distribution in adjacent cells

We first focus on a single-cell scenario, where K users upload packets to one UAV, and then study the impacts of UAV density on the required total bandwidth for URLLC.

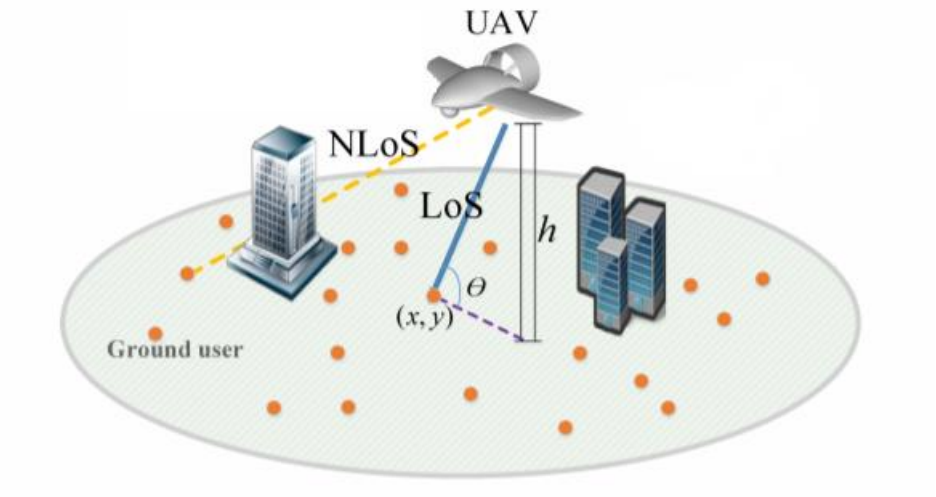

Figure 11 System model with LoS and NLoS [8]

The table 3 represents the definition or the abbreviation with their respective notations.

Table 3 Definition and notation

Definition	Notation
Number of UAVS	k
Altitude of UAV	h
Minimum Altitude of UAV	h_{min}
Maximum Altitude of UAV	h_{max}
Elevation Angle	θ_k
Large scale channel gain	$\alpha_k^{\sim\xi}$
Small scale channel gain	$f_{gk}(z)$
Signal to Noise Ratio	γ
Packet Size	b_k
Carrier frequency	f_c
Required packet loss probability	ε_{max}
Bandwidth	W_k

Channel coherence bandwidth	W_c
Horizontal distance between AP & UAV	R_k
Distance between AP & UAV	d_k
Network availability	P_A
Network availability requirement	P_A^{req}
Transmit power	P_k
Single-sided noise spectral density	N_0
Transmission delay	D_t
Achievable data Rate	R_k^{ξ}
Channel dispersion	V_k
Decoding error probability	ε_k^{ξ}
Indicator function of the LoS path	ξ

In order to analyse the effect of the UAVs altitude on the provided service, the researcher have defined the service threshold in terms of the maximum allowable pathloss PL_{max}. When the total pathloss between the UAV and a receiver exceeds this threshold, the link is deemed as failed.

For ground receivers, this threshold translates into a coverage disk (zone) of radius *R*, since all receivers within this disk have a pathloss that is less than or equal PL_{max}. The cell radius of the coverage zone can be written as [10]:

$$R = r|_{\wedge = PL_{max}} \tag{21}$$

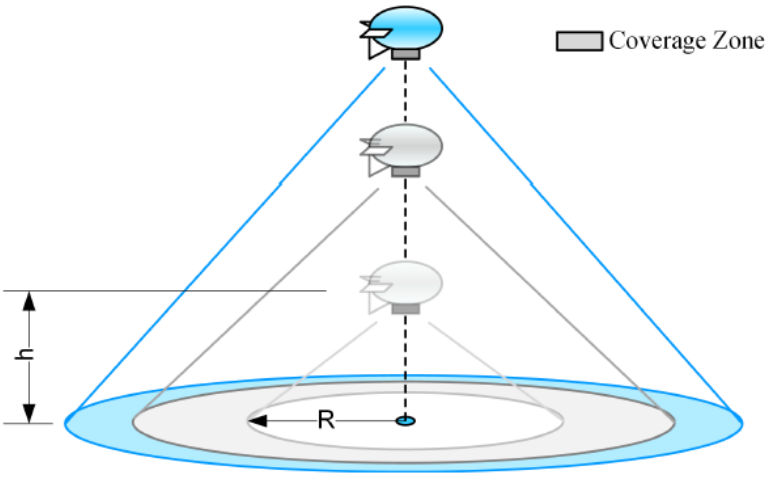

Figure 12 Fixing the altitude for the best coverage

Accordingly, the optimization problem is to find the best altitude that will maximize *R* as shown in figure 12. In order to do that, we use a relation between the UAV altitude *h* and the cell radius *R*. By rewriting the equation, we have:

$$PL_{LOS} = \ 20\,log\,d + 20\,log\,f + 20\,log\left(\frac{4\pi}{C}\right) + \ \eta_{LOS} \qquad (22)$$

$$PL_{NLOS} = 20\,log\,d + 20\,log\,f + 20\,log\left(\frac{4\pi}{C}\right) + \ \eta_{NLOS} \qquad (23)$$

where

d - distance between UAV & AP at a circle of radius *r*.
d - $\sqrt{h2\ +\ r2}$
f - system frequency.
η_{LOS} and η_{NLOS} - path loss (in dB).

In general, η_{NLOS} is larger than η_{LOS} due to the more severe attenuation associated with NLoS.

The FSPL is according to Friis equation with the assumption of isotropic transmitter and receiver antennas.

$$\wedge = \ P(LOS) * PL_{LOS} + \ P(NLOS) * PL_{NLOS} \qquad (24)$$

we know that θ = arctan (h / r). After performing some simple algebraic reductions, the equation can be written as ,

$$PL_{max} = \frac{A}{1 + a\,exp\left(-b\left[arctan\frac{h}{R} - a\right]\right) + 10log(h^2 + R^2) + B} \qquad (25)$$

Where,

A - ηLoS - ηNLoS
B - 20 log f + 20 log(4π/c) + ηNLoS

The above equation 25 is implicit, where neither *R* nor *h* can be written as an explicit function of each other. In order to obtain the optimum altitude of the UAV *h* that yields the best coverage, we need to search for the value of *h* that satisfies the equation of the critical point [10]:

$$\frac{\partial R}{\partial h} = 0 \tag{26}$$

i.e., the point at which the radius-altitude curve changes its direction. The optimum altitude of a UAV is strongly dependent on the specific urban environment condition.

It is important to note that the value of PL_{max} depends on the sensitivity of the receiver, communication technology, and the target quality of service. It is observed that for large values of $PL_{max,}$ the optimum altitude may exceed the earth's atmosphere which is not a practically viable solution. Since we mainly consider UAVs in LAP and LAPs will have physical constraints for reaching a maximum altitude, the optimum altitude for the UAV hence can be the found by imposing a constraint on h in the proposed model [10].

4.1 Large scale channel gain

Let α_k be the large-scale channel gain of the kth user, where ξ is an indicator function of the LoS path. If there is a LoS path, then ξ = 1. Otherwise, ξ = 0. Then, α_k can be obtained from the following expressions,

$$-10log_{10}\alpha_k^{\xi} = 20\,log\,d_k + \alpha_0 + \eta^{\xi}(\theta_k) \tag{27}$$

where α_0 = 20 log10 f_c - 27.55 is determined by carrier frequency f_c (MHz), and $\eta^{\xi}(\theta_k)$ is a normally distributed random variable, which reflects the location variability of the UAV and shadowing,

$$\eta^{\xi}(\theta_k) \sim N\left(\mu_{\xi}, \sigma_{\xi}^2((\theta_k)\right) \tag{28}$$

With LoS path, the standard deviation of shadowing is smaller than that without LoS path. As shown, the relation between the standard deviation and the elevation angle can be fitted as

$$\sigma_{\xi}(\theta_k) = a_{\xi}\, exp\left(-c_{\xi}\theta_k\right) \tag{29}$$

where a_{ξ} and c_{ξ} are parameters depending on the types of communication environments [2].

4.2 Small scale channel gain

Fading can be either small or large. Large fading is related to the distance between the transmitter and the receiver. Small fading is related to the rapid fluctuation of fading according to the position. It describes how the amplitude of the channel changes when m>1.

When m =1, probability distribution function is Rayleigh. It holds for all values of Z (from zero to infinite). Z is the random variable that provides the amplitude of the channel.

We consider that small-scale channel fading follows Rician fading when there is LoS path, and follows Rayleigh fading when there is no LoS path , which can be unified as Nakagami-m channel with different values of m. Denote the small-scale channel gain of the kth user as g_k. Then, the probability density function is given by

$$f_{gk}(z) = \frac{m^m z^{m-1}}{(m-1)!} exp(-mz) \quad (30)$$

When there is LoS path, m > 1. Otherwise, m = 1 [1].

4.3 Reliability and Network Availability

In this section, I have described and provided the expressions of the decoding error probability and the UL network availability.

4.3.1 Decoding error probability

As it was discussed earlier, the k^{th} user transmits a packet with b_k bits to the UAV with some certain transmission delay D_t, which is same as the transmission duration. D_t is smaller than channel coherence time, which is the typical scenario for URLLC.

In order to satisfy the reliability requirement, the decoding error probability should not surpass ε_{max}. To avoid the large overhead in the channel, retransmission is not applicable, and channel state information (CSI) is not assumed available at each user. However, by transmitting pilots, CSI is available at the UAV.

With short transmission duration, the block length of channel codes is short. The assumption has been made that each packet is transmitted over a flat fading channel. The achievable rate in short block length regime under such quasi-static flat fading channel can be approximated by [1],

$$R_k^{\xi} \approx \frac{W_k}{ln\,2}\left[ln(1+\gamma) - \sqrt{\frac{V_k^{\xi}}{D_t W_k}} f_Q^{-1}\left(\varepsilon_k^{\xi}\right)\right] \quad (31)$$

where,

$$\gamma = \frac{\alpha_k g_k p_k}{N_0 W_k}; \tag{32}$$

γ - Signal to Noise Ratio
W_k - Allocated bandwidth
P_k - Transmitted power of the kth user
N_0 - Single-side noise spectral density
f_Q^{-1} - Inverse of Q-function
ε_t^{ξ} - Decoding error probability
V_k^{ξ} - Channel dispersion

$$V_k = 1 - \frac{1}{(1+\gamma)^2}; \tag{33}$$

The decoding error probability to send a packet from the user to the UAV with some certain transmission duration can be obtained by fixing $D_t R_k^{\xi} = b_k$,

$$\varepsilon_k^{\xi}\left(\alpha_k^{\xi}\right) \approx \mathbb{E}_{gk}\left\{ f_Q\left(\sqrt{\frac{D_t W_k}{V_k^{\xi}}} \left[ln(1+\gamma) - \frac{b_k \, ln\, 2}{D_t W_k} \right] \right) \middle| \alpha_k^{\xi} \right\}; \tag{34}$$

where the average is taken over small-scale channel gain conditioned on the large-scale channel gain.

Thus, the reliability can be satisfied if,

$$\varepsilon_k^{\xi}\left(\alpha_k^{\xi}\right) \leq \varepsilon_{max} \; for \;\; \xi = 0{,}1 \tag{35}$$

Therefore, decoding error probability should not exceed ε_{max} in any case.

4.3.2 Network availability

Network availability is defined as the probability that the round-trip delay and the overall reliability requirement can be satisfied. Let P_A be the network availability. Then, the network availability of our system can be given as,

$$P_A = Pr\left\{ \varepsilon_k^1 \alpha_k^{\xi} \leq \varepsilon_{max} \right\} P_k^L + Pr\left\{ \varepsilon_k^0 \alpha_k^{\xi} \leq \varepsilon_{max} \right\} (1 - P_k^L) \tag{36}$$

It is easy to say that $\varepsilon_k^{\xi} \alpha_k^{\xi}$ decreases with α_k. With the help of binary searching, we can find two thresholds for largescale channel gain that can satisfy $\varepsilon_k^{\xi} \alpha_k^{\xi} = \varepsilon_{max}$. We denote the two thresholds as $\tilde{\alpha_k^{\xi}}, \xi = 0{,}1$.

Then, the reliability requirement can be satisfied if and only if, $\alpha_k^{\sim\xi} \geq \alpha_k^{\sim\xi}$

As a result, the network availability can be re-expressed as

$$P_A = Pr\{\alpha_k^1 \geq \alpha_k^{\sim 1}\} P_k^L + Pr\{\alpha_k^0 \geq \alpha_k^{\sim 0}\} \left(1 - P_k^L\right) \quad (37)$$

After solving,

$$Pr\left\{\alpha_k^{\xi} \geq \alpha_k^{\sim\xi}\right\} = 1 - f_Q\left(\frac{-10log_{10}\alpha_k^{\sim\xi} - 20\,log\,d_k - \alpha_0 - \mu_\xi}{\sigma_\xi(\theta_k)}\right) \quad (38)$$

By substituting this equation 38 into equation 37, the network availability can be obtained.

4.4 UAV deployment and bandwidth allocation

4.4.1 Problem Formulation

We try to minimize the total bandwidth required to guarantee the QoS and network availability for serving URLLC in a UAV network by optimising the altitude with the help of frequency reuse factor F_R. The network availability should be greater than the required network availability and it should also satisfy the altitude.

It should also satisfy the below constraints,

$$\varepsilon_k^{\xi}(\alpha_k^{\sim\xi}) = \varepsilon_{max},\ k = 0, 1, 2, \ldots K \quad (39)$$

$$0 \leq W_k \leq W_c,\ k = 0, 1, 2, \ldots K \quad (40)$$

where,

W_c - Channel coherence bandwidth.
ε_{max} - Maximum decoding error probability.

The coherence bandwidth W_c depends on the communication environment and carrier frequency, which are known in advance. As there is a trade-off between the bandwidth, altitude, and the required large-scale channel gain, it is very tough to find the optimal solution to the problem.

In the view of cell-edge user requires the largest bandwidth, we first minimize the required bandwidth of a cell-edge user by optimizing h. Then, we fix h and minimize the bandwidth required by the other users.

After obtaining the optimal altitude, we can find the minimal bandwidth required by the other users from the following problem by satisfying the constraints.

4.4.2 Feasibility of the Problem

The optimization problem that maximizes network availability can be formulated as follows, $\alpha_i^{\sim\xi}$ decreases with W_i. Moreover, $Pr\left\{\alpha_i^{\xi} \geq \alpha_i^{\sim\xi}\right\}$ decreases with $\alpha_i^{\sim\xi}$.

Therefore, the maximal network availability is achieved when the equality coherence bandwidth is equal to the required bandwidth. When the bandwidth is given, the required large-scale channel gain that satisfies can be obtained via binary searching.

The expression of P_A in equation (37) is very complex to obtain any useful insight. To overcome this difficulty, we consider the following approximation: when there is no LoS path, the QoS of a user can hardly be satisfied, i.e., $Pr\{\alpha_i^0 \geq \alpha_i^{\sim 0}\} \approx 0$. Let us evaluate this approximation via numerical results. The approximated network availability in equation (37) can be re-written as,

$$P_A \approx Pr\{\alpha_i^1 \geq \alpha_i^{\sim 1}\} P_i^L \tag{41}$$

Maximizing the network availability is equivalent to minimizing,

$$1 - P_A = 1 - Pr\{\alpha_i^1 \geq \alpha_i^{\sim 1}\} P_i^L \tag{42}$$

$$1 - P_A = (1 - P_i^L) + (1 - Pr\{\alpha_i^1 \geq \alpha_i^{\sim 1}\}) P_i^L \tag{43}$$

To achieve high P_A that is close to one, both $Pr\{\alpha_i^1 \geq \alpha_i^{\sim 1}\}$ and P_i^L in equation (43) should be close to one. With $P_i^L \approx 1$, equation (42) can be accurately approximated by

$$1 - P_A \approx (1 - P_i^L) + (1 - Pr\{\alpha_i^1 \geq \alpha_i^{\sim 1}\}) \tag{44}$$

With the approximation in (44) can be obtained by solving the following problem,

$$\min_{d_i} (1 - P_i^L) + (1 - Pr\{\alpha_i^1 \geq \alpha_i^{\sim 1}\}) \tag{45}$$

$$such\ that \quad \sqrt{R_i^2 + h_{min}^2} \leq d_i \leq \sqrt{R_i^2 + h_{max}^2} \tag{46}$$

$$P_i^L \geq P_A^{req} \ \&\ Pr\{\alpha_i^1 \geq \alpha_i^{\sim 1}\} > P_A^{req} \tag{47}$$

where $d_i \leq \sqrt{R_i^2 + h^2}$

constraint (46) is equivalent to constraint on the height, constraints on the network availability and $W_i = W_c$ are used to obtain $\tilde{\alpha_i^{-1}}$.

4.5 Simulation results of UAV-Assisted Uplink Transmission

In this section, I have provided the simulation results that were obtained for the PLoS, the network availability and the bandwidth optimisation.

4.5.1 Probability of LoS vs the defined set of Theta (for different environments)

Figure 13 depicts the variation of PLoS with respect to the elevation angle as per equation (6) for all four different environments such as Suburban, Urban, Dense-urban, and High-rise scenarios.

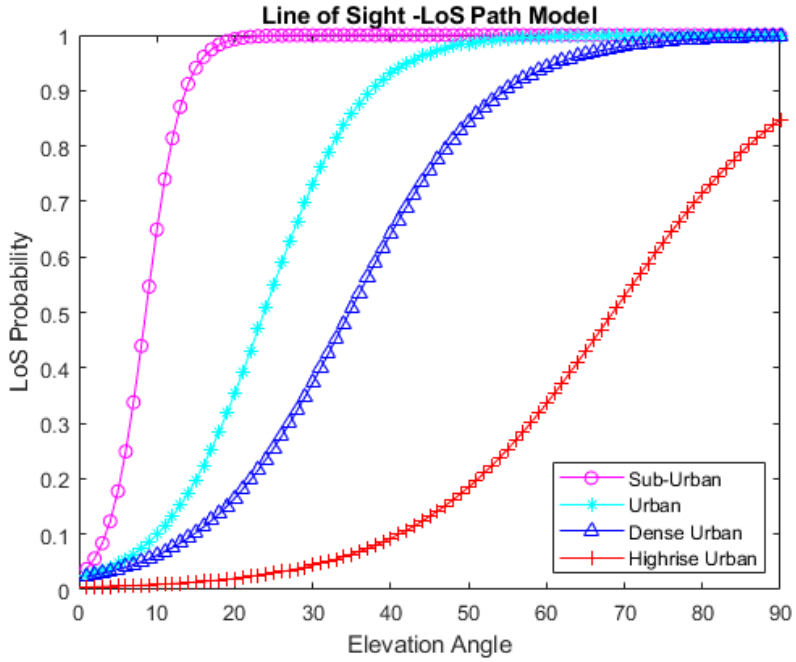

Figure 13 PLoS vs Elevation Angle

As the density of tall buildings is the least in Sub-urban areas which is why it is less complicated to attain a direct LoS. On the contrary, the graph adequately depicts that high-rise urban areas have less LoS probability due to the obstruction created by high-rise or tall buildings or any objects that act as an obstacle in the downtown areas.

4.5.2 Probability of LoS vs UAV altitude (for different environments)

Figure 14 depicts the variation of PLoS with respect to the altitude of the UAV as per equation (6). The graph shows, decrease in LoS probability as the height of buildings increases from suburban to urban, graduating to dense urban and then finally to high-rise urban environments.

The graph also exhibits that the probability of LoS is not reaching '1' for high-rise urban areas. It is never satisfied because we have obstacles, shadowing, and fading components when the building size increases. This is the main motivation behind implementing the AF relay in the proposed work to achieve the PLoS for high-rise environments.

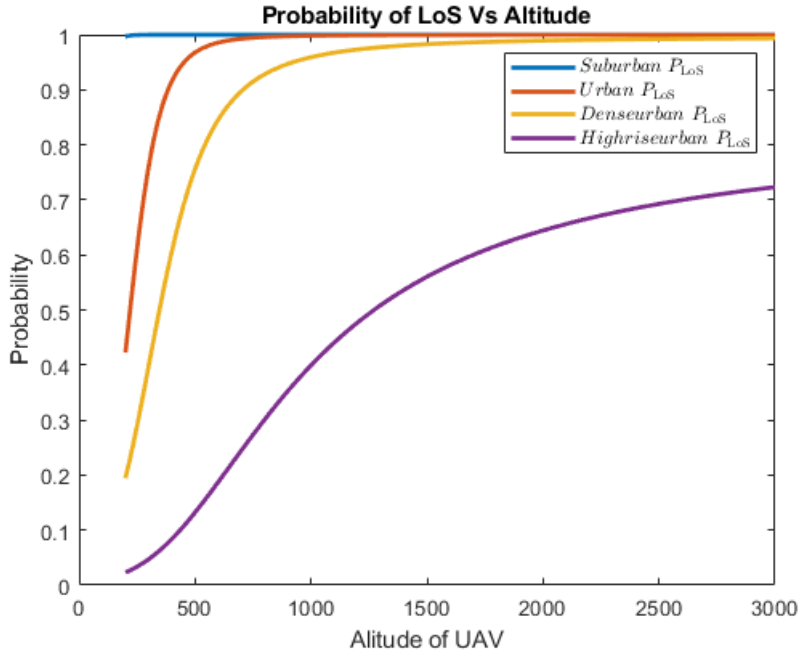

Figure 14 PLoS vs UAV Altitude

4.5.3 Simulation of network availability

Figure 15 depicts the variation of probability of network availability with respect to the altitude of the UAV as given by equation (41) and equation (44) for approximate and accurate respectively. The probability of direct LoS goes hand in hand with the probability of network availability and thus these graphs explain the same phenomenon that- increase in LoS increases the probability of network availability.

In the case of high-rise urban environment, the approximations in (41), $Pr\{\alpha_k^0 \geq \tilde{\alpha_k^0}\} \approx 0$, and $\sigma_1(\theta_k)$ are validated. The results show that the approximation is very accurate with different h. Since $1 - \Pr\{\alpha_k^0 \geq \tilde{\alpha_k^0}\}$ is very close to 1, $Pr\{\alpha_k^0 \geq \tilde{\alpha_k^0}\} \approx 0$, is also very accurate. Moreover, $1 - \Pr\{\alpha_k^0 \geq \tilde{\alpha_k^0}\}$ is obtained when $\sigma_1(\theta_k)$ varies with θ_k according to (37). The results show that such a simplification

does not change the convexity of $Pr\{\alpha_k^1 \geq \alpha_k^{\sim 1}\}$ when $Pr\{\alpha_k^1 \geq \alpha_k^{\sim 1}\}$ is small. The approximations are also accurate with different R_k and W_k [1].

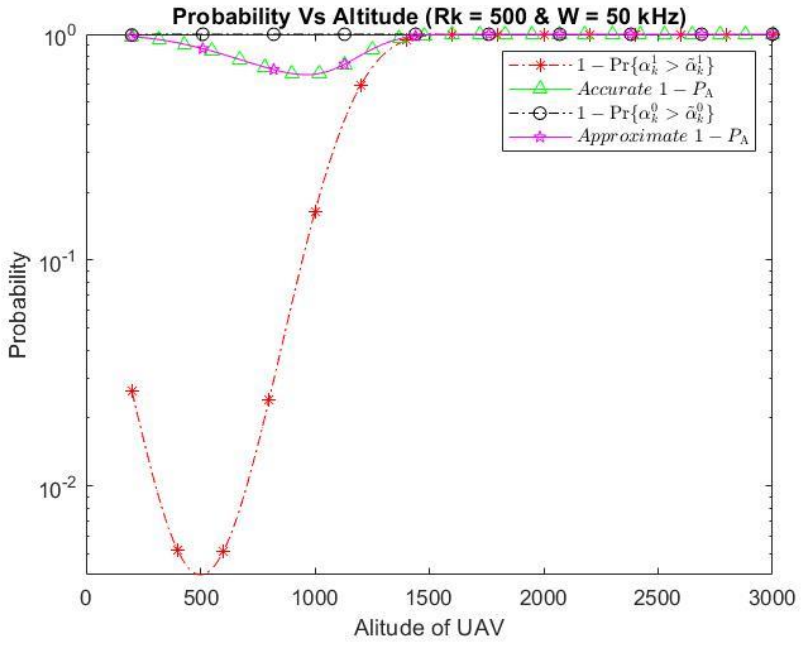

Figure 15 Network availability before relay

4.5.4 Bandwidth Optimization

In order to analyse the bandwidth required to serve the URLLC in a UAV network, we first minimize the total bandwidth required to guarantee the QoS and network availability.

We can observe different graphs for the bandwidth of 50 kHz and 60 kHz for the high-rise environment. The same can be applied to the other environments. The optimum bandwidth can be found by the numerical search. We can apply the optimization problem to reduce the bandwidth without compromising the latency and the network availability.

Let us observe from the below graphs what happens to the network availability graph when the bandwidth changes. Figure 15 shows the network availability graph with a bandwidth 50 kHz. Figure 16 depicts the network availability graph with the bandwidth 60 kHz for the same environmental condition.

The 1- $Pr\{\alpha_k^1 \geq \alpha_k^{\sim 1}\}$ has the probability of 10^{-2} in case of less bandwidth, whereas the probability is close to 10^{-8} when the bandwidth increases. The approximate and the accurate network curves have some impact when the bandwidth changes. This shows that choosing the right bandwidth is also an important factor in to achieve the system requirements.

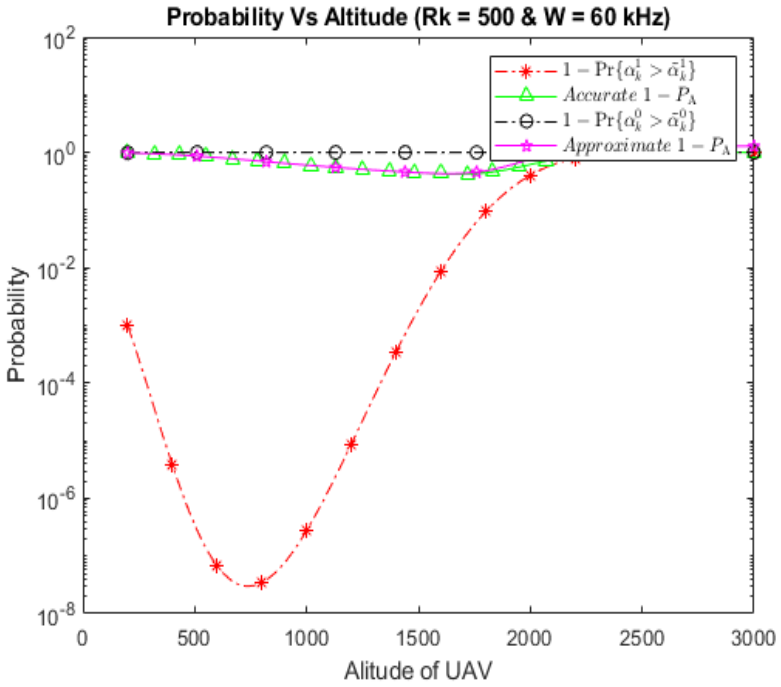

Figure 16 Bandwidth 60kHZ for high-rise urban

4.6 Conclusion on UAV-Assisted Uplink Transmission

In this system, we have seen how they have characterized the latency, reliability, and network availability of URLLC in UAV communication systems and optimized the altitude of UAVs and the bandwidth allocation that minimizes the required total bandwidth of URLLC for a given density of UAVs. Analysis showed that the probability of LoS path and the network availability is strictly concave in the communication distance between a ground user and a UAV.

UAV can only provide high network availability for URLLC in suburban areas. This implies that in other types of communication environments, more than one ground-to-air or ground-to-ground link is needed. In the proposed research, we work on the idea of implementing the AF protocol as a relay between the transmitter and the main UAV, to increase the probability of line of sight and to achieve high network availability by reducing the latency in other environments (especially for high rise urban environment).

5 Proposed relay facilitated URLLC UAV system

As discussed in the last chapter, even with a single UAV, it is difficult to establish a stable data link when obstacles such as trees, tall buildings, or mountains separate UAV and GCS in the high-rise urban scenario. The use of a communication relay system provides a practical way to solve these problems, improving the performance of UAV communication in BLoS and cross-obstacle operations [17].

However, it can be difficult to achieve the PLoS and network availability for critical URLLC applications with only one UAV deployed, while keeping cost and system complexity requirements met. To harness the advantages of UAVs in these situations and minimize the drawbacks at the same time, an alternative solution is to deploy a multi-UAV system, which could utilize the inter-connectivity among multiple UAVs to maintain uninterrupted communication between every UAV and the ground control station.

In this proposed model as illustrated in figure 17, a UAV communication relay solution has been developed, which uses AF relay and routing to extend the communication range and bypass obstacles at a low cost. The objective is to develop two-UAV system that demonstrated the ability to relay radio communication. This system consists of two UAVs (One UAV on the rooftop as a relay, other as flying UAV), but its design could accommodate the addition of more UAVs [18].

The system uses the additional relayed UAV as a communication relay point and enables the other UAV to operate in areas where direct communication with ground control cannot be established. This configuration allows communication to be established across obstacles or over a distance exceeding the range of the onboard radio transceiver.

Our design aims at data transmission from a source to a destination node via the well-known AF protocol. AF relay performs better than the Decode and Forward relay (DF) when the number of channels blocklength is small [19]. It is beneficial to adopt the AF relay when the latency requirement is stringent, which is usually the case in URLLC applications [19].

Let us assume that a link between a source and a destination node of *Tx* and *Rx* antenna has no direct path [20]. The relay receives the information from the source and then forwards its amplified version to the destination as shown in figure 18. The reliability of the UAV relay was analysed in terms of network availability and latency.

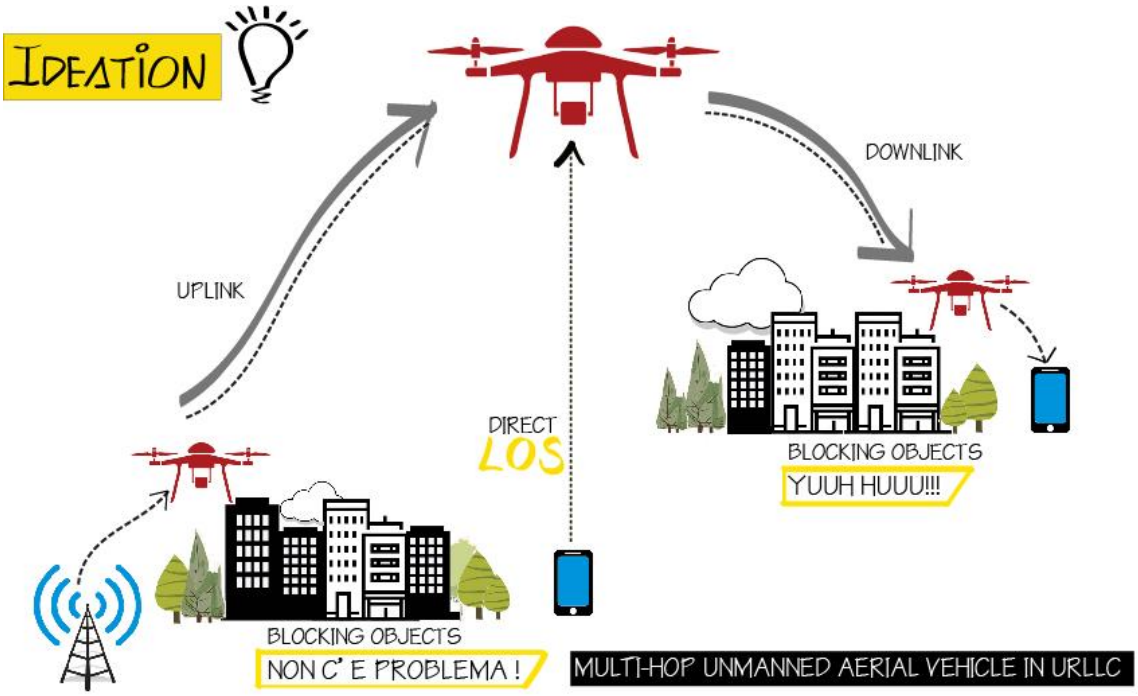

Figure 17 Proposed system model.

Figure 18 Source to destination flow with AF relay

However, additional processing time may be required for the AF mode, which can compromise stringent delay requirement of URLLC applications. We jointly optimize bandwidth and altitude to minimize the decoding error probability, where the relay is operating under the AF mode without the signal processing delay. The decoding error probability under short blocklength is adopted. We can observe that the decoding error probability is a monotonically decreasing function of the SNR.

It is important to note that the channel model from the source to the UAV is assumed to be high-rise urban environment.

5.1 Optimum placement of UAV as relays

Our main focus is on the specific problem of UAV positioning, which is known to crucially affect performance. In this part, we study the optimum altitude of the UAV as a relaying station using realistic UAV channel models and numerical search by focusing on the reliability metrics in terms of power loss, outage probability and BER. Both UAV on the side of the rooftop of a building and mobile UAVs are considered.

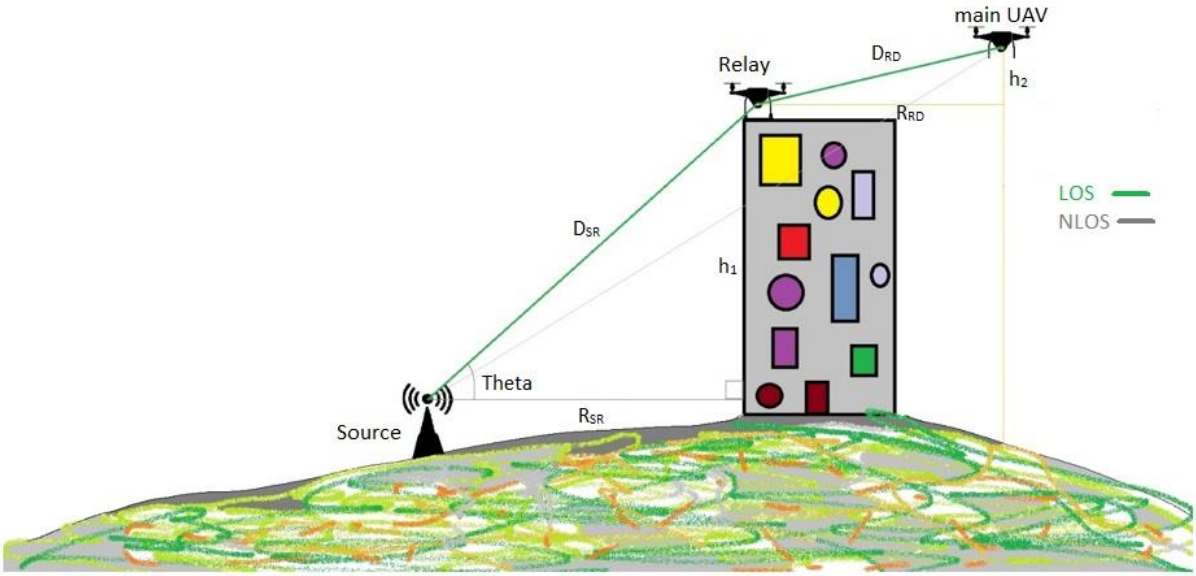

Figure 19 System model with relay

One challenge in UAV communications is the flight time constraint of UAV. The system model is delineated in such a way as to act robustly in all environmental conditions, also considering the power condition of the UAV. For instance, the UAV is controlled by an optimal control model to tackle the battery related issues. Considering the power of the UAV as an important factor that must overcome the efficiency loss due to low battery level, the 2nd replacement UAV will be replaced with the active UAV when the battery level drops less than 10 %.

Another important issue is the placement of the UAV. Several researchers have worked on the optimum placement of UAVs as aerial base stations. The relayed UAV which acts as a relay between the GCS and the main UAV is static, it is fixed on the side of the rooftop of a building with an altitude of h_1 above the ground. The main UAV is mobile, when the UAV moves with some certain altitude h_2 straight towards the user, the number of obstacles between the UAV and the user keeps decreasing and the channel gain improves [21].

Consider that the heights h_1 and h_2 (in figure 19) are large enough such that there is always LoS propagation between the BS and the UAV. The signal propagation by optimising the altitude makes the LoS yields a higher channel gain compared to the NLoS scenario [22].

The base station/source is located R_{SR} meters away from the obstacle/building which blocks the LoS from the main UAV, which stands at the height of h_1. It is necessary for the UAV to stay on top of the building to always have the probability of LoS equals 1. Users inside the cell are expected to have better performances. In the case of multiple users, orthogonal channels can be used to avoid co-channel interference. Even with the inclusion of relay, it follows the same ground to air pathloss propagation model.

As shown in figure 20, The distance (D_{SR}) from the source to relay is calculated with the formula,

$$D_{SR} = \sqrt{R_{SR}^2 + h_1^2} \tag{48}$$

Large scale channel gain is calculated for the measured distance and then, SNR will be computed for the first link.

Similarly, the distance of the relay (D_{RD}) from the building and having some approximation of the main drone height, the horizontal distance from the relay to destination is calculated with the formula,

$$D_{RD} = \sqrt{R_{RD}^2 + h_2^2} \tag{49}$$

Large scale channel gain is calculated for the measured distance and then, SNR will be computed for the second link.

Finally, Overall SNR is computed by combining the SNR of both the links and this will be implemented in the non-line of sight equation to improve the efficiency.

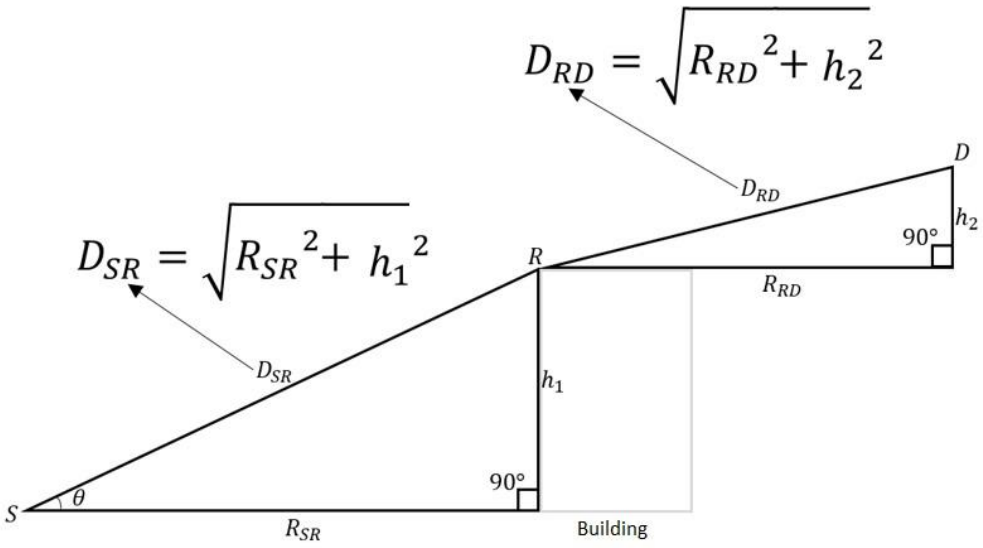

Figure 20 Distance calculation (for SR & RD)

5.2 Calculation of SNR for AF relay

With AF as a relay, the UAV receives the information from the ground user and forwards it to the remote station without any further processing or the other way around if the remote station transmits data.

In the general case, SNR is given as,

$$\gamma = \frac{\alpha_k g_k p_k}{N_0 W_k}; \quad (50)$$

where,

$\alpha_k - Large\ scale\ channel\ gain$
$g_k - Small\ scale\ channel\ gain$
$N_0 - Single\ side\ noise\ spectral\ density$
$W_k - Bandwidth$
$p_k - Power$

In the case of AF relay, the inverse of the overall SNR is the sum of the inverse of SNRs on the two links. Computation of the SNR will be given as the input to the relay. The large scale and small-scale channel gain only differ. Other components remain the same.

The new overall SNR is given by,

$$\frac{1}{\gamma_{tot}} = \frac{1}{\gamma_{S-R}} + \frac{1}{\gamma_{R-D}}; \quad (51)$$

$$SNR_{tot} \leq \min (SNR_{SR}, SNR_{RS})$$

where

$\gamma_{S-R} - SNR\ from\ source\ to\ relay$.
$\gamma_{R-D} - SNR\ from\ relay\ to\ destination.$
$\gamma_{tot} - Total\ SNR$

$SNR\ from\ source\ to\ relay$ is given by,

$$\gamma_{S-R} = \frac{\alpha_{S-R} g_k p_k}{N_0 W_k}; \quad (52)$$

$SNR\ from\ relay\ to\ destination$ is given by,

$$\gamma_{R-D} = \frac{\alpha_{R-D} g_k p_k}{N_0 W_k}; \quad (53)$$

$\alpha_{S-R} - Large\ scale\ channel\ gain\ (Source\ to\ Relay)$.
$\alpha_{R-D} - Large\ scale\ channel\ gain\ (Relay\ to\ Destination)$.

$$\frac{1}{\gamma_{tot}} = \frac{1}{\frac{\alpha_{S-R} g_k p_k}{N_0 W_k}} + \frac{1}{\frac{\alpha_{R-D} g_k p_k}{N_0 W_k}};$$

$$\frac{1}{\gamma_{tot}} = \frac{N_0 W_k}{\alpha_{S-R} g_k p_k} + \frac{N_0 W_k}{\alpha_{R-D} g_k p_k};$$

$$\frac{1}{\gamma_{tot}} = \frac{N_0 W_k}{g_k p_k}\left(\frac{1}{\alpha_{S-R}} + \frac{1}{\alpha_{R-D}}\right);$$

The final SNR with AF relay is,

$$\frac{1}{\frac{N_0 W_k}{g_k p_k}\left(\frac{1}{\alpha_{S-R}} + \frac{1}{\alpha_{R-D}}\right)} = \gamma_{tot} \quad (54)$$

With the new calculated SNR, the large-scale channel gain model changes. The large-scale channel gain model in the case of AF relay will be,

$$-10log_{10}\alpha_{S-R} = 20log_{10}d_{S-R} + \alpha_0 + \eta(\theta_k); \quad (55)$$

$$-10log_{10}\alpha_{R-D} = 20log_{10}d_{R-D} + \alpha_0 + \eta(\theta_k); \quad (56)$$

We can observe that the large-scale channel gain model changes as per the new distance calculation from the source to the relay and the relay to the main UAV.

As the SNR has a huge positive impact with the help of relay, SNR term (γ) in channel rate and the decoding packet error rate from the equations 31, 33 and 34 will be changed according to the calculated new SNR γ_{tot}.

5.3 Distribution of building heights

In the majority of cases, the high-rise environment affects the wireless communication services notably in the LoS. Problems are more likely to occur if a building or structure is constructed significantly taller than those around it, or it is on high ground. In general, a wireless service works best if there is a clear path between the source and the intended destination without any shadow zone.

To overcome the shadow zone (Figure 21) of a taller building and the corresponding NLoS, the relay must be placed on a certain elevation, which in turn will drastically improve the LoS at the destination point. Moreover, this particular elevation has to be calculated accordingly without any vague assumptions.

We have explained the height distribution in downtown areas. Firstly, the raw building elevation must be analysed to derive the building height statistics and create a detailed

histogram showing the overall distribution of the heights based on several terrain conditions such as “residential, commercial, industrial, downtown, etc.”

Following this, the proper challenging environment must be considered for the above-mentioned terrain conditions, in our case we went along choosing “Los Angeles” which is considered as a “High-rise environment”, where all the terrain conditions (type of building areas) will be satisfied. Furthermore, the city has the highest variability in building heights and contains the tallest buildings.

The main source of the building height of this particular environment was gathered from a civil engineering published article [21], where the datasets for the city from the southern California Association of Governments (SCAG) [21] and Maricopa Association of Governments (MAG) [21].

Note: The resolution of the information dataset is around 6-inch pixel size approx.

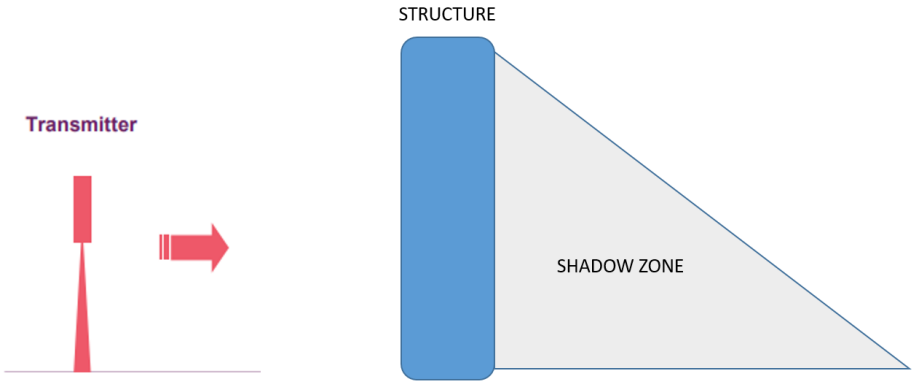

Figure 21 Shadow zone

Table 4 Building height characteristics.

	Los Angeles	TIER		
No of Buildings	3.353		Residential (%)	6,4
Area (km^2)	12		Commercial (%)	28,5
Avg. Height (m)	12		Industrial (%)	6,3
Std. Dev (m)	22,7		Mixed & trans. (%)	15,3
Max. Height (m)	331		Urban & Built up (%)	19,4
			Downtown (%)	45

The table 4 represents the data of the terrain conditions and the corresponding percentage of the buildings situated on each of the conditions. It is also clear from the table that the majority of the buildings come under the commercial terrain condition which will also be our point of interest to calculate the line of sight for this particular environment.

Table 5 Building height distribution.

LOS ANGELES COMMERCIAL BUILDINGS					
	Height Distribution	# of Buildings	Range (m)	AVG. HEIGHT DISTRIBUTION	Min - Avg. - Max (m)
Cluster - 1	0 to 5	277	0 to 331		0>2.5>5
Cluster - 2	5 to 10	201			5>7.5>10
Cluster - 3	10 to 15	67			10>12.5>15
Cluster - 4	15 to 25	153			15>20>25
Cluster - 5	25 to 50	172			25>37.5>50
Cluster - 6	50 to 100	57			50>75>100
Cluster - 7	100 to 200	19			100>150>200
Cluster - 8	200 to 400	9			200>300>400
Total number of buildings		955			

Table 5 represents the detailed building height distribution from the total number of buildings in the commercial terrain condition. The height ranges are divided into 8 clusters and the average height is calculated for each of the clusters accordingly.

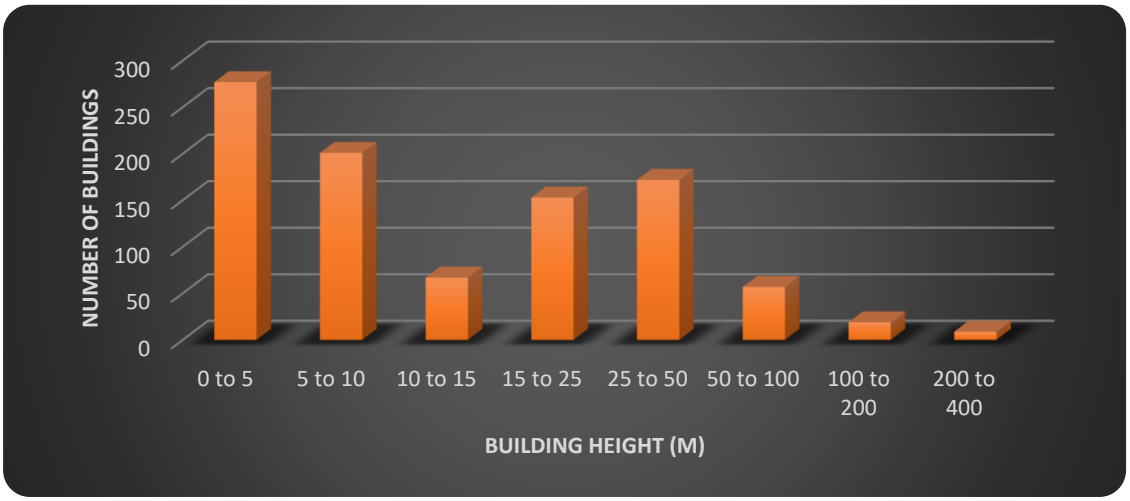

Figure 22 Building height histogram.

The histogram of the building height has been grouped as per different environment height. For example, the building from the height range of 0 to 5 meters and 5 to 10 meters can be categorized under the suburban environment. Similarly, the building from the height range of 10 to 15 meters and 15 to 25 meters can be categorized as urban environment and so on. The table 6 depicted that the percentage calculation for each cluster category of the height distribution and a detailed histogram is furnished based on the calculated percentage of the heights with respect to these clusters (*refer to figure 22*).

Table 6 Weightage on the height distribution

	Height Distribution (in meter)	Percentage%
Cluster - 1	0 to 5	29,0052356
Cluster - 2	5 to 10	21,04712042
Cluster - 3	10 to 15	7,015706806
Cluster - 4	15 to 25	16,02094241
Cluster - 5	25 to 50	18,0104712
Cluster - 6	50 to 100	5,968586387
Cluster - 7	100 to 200	1,989528796
Cluster - 8	200 to 400	0,942408377
Total		100

As the distribution of the building height is well known, we fix the relay facilitated UAV on the corner of the rooftop of a building as per data on the building height. Then we rescale the height of the relay as the new ground level of the UAV. By rescaling the UAV height as the new ground level, the view of the main UAV from the relay UAV becomes lower. Thereby, the probability of LoS with the main UAV is calculated.

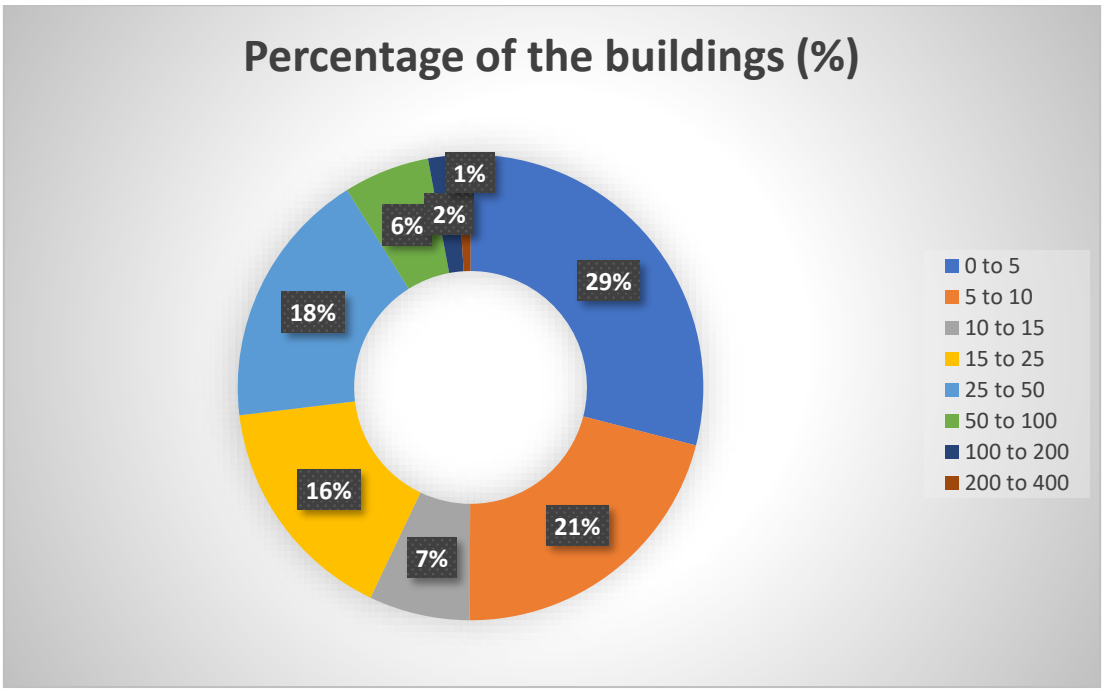

Figure 23 Pie chart view of building distribution

It is important to note that the height of the main UAV will be at least as tall as the maximum height of the building in the specific environment. This means that the height of the main UAV can be anywhere above the building.

Below figures 24 and 25 is an example that shows 2 different cases in fixing the relay at the optimum altitude or the right location.

In case 1, The relay is placed on the corner of building 1, which amplifies the signal and sends it to the mobile UAV. As the relay creates two links (one from MU to relay and the other from the relay to mobile UAV), it increased the chances of LoS. Hence the network availability requirement is fulfilled.

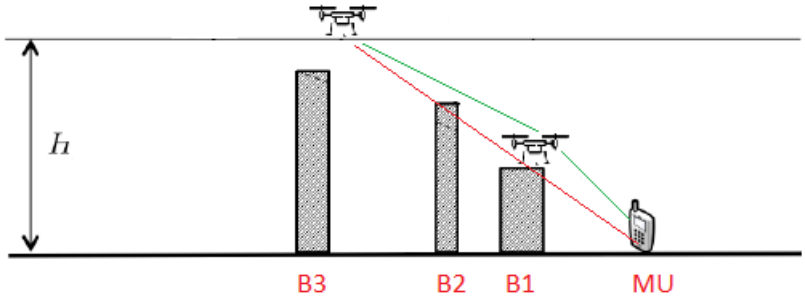

Figure 24 Case 1: LoS with relay

In case 2, The relay is still placed on the corner of building 1. However, the position of the mobile UAV is far from the relay. We can observe that building 2 (B2) stands as an obstacle and it has NLoS in the second link. Therefore, we are unable to achieve the LoS.

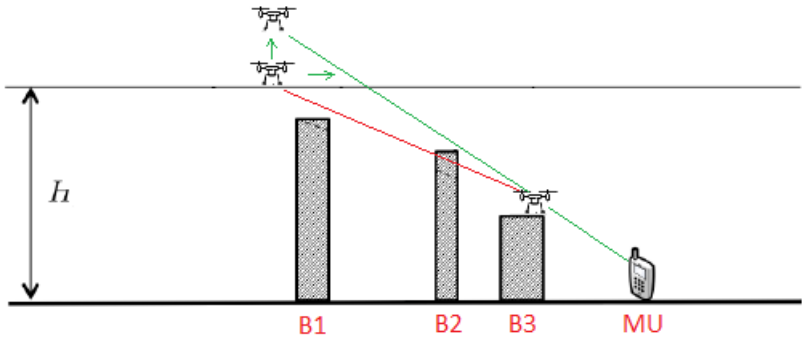

Figure 25 Case 2: NLoS with relay

However, If the mobile UAV bit higher than the current position or if it is towards the relay, it may probably enter from NLoS to LoS. Increasing the height of the main UAV always has a good impact on achieving the LoS. This figure clearly shows the importance of choosing the right altitude or location for placing the relay and UAV. Thus, altitude plays a crucial part in achieving the LoS.

Note: In order to find the right place to fix the mobile UAV with some certain height and to keep the relay, the data on the building height distribution needs to be collected for the selected area.

5.3.1 Calculation of PLoS with AF relay

Once the data of the distribution of building height is collected, we fix the UAV position and altitude of the relay as per the optimisation algorithm. Referring to table 6, we find the probability of LoS for the specific cluster with the percentile of the building i.e, the fraction of the building. We can name the weightage about the fraction of building as W1,W2… Wn. Then, PLOS of each cluster or the environment will be the product of the weightage times the line of sight in the particular cluster.

$$\mathrm{P}_{\mathrm{new}}^{1} = \mathrm{W}_{1} * \mathrm{P}_{\mathrm{LOS}}^{1}$$

Similarly,

$$\mathrm{P}_{\mathrm{new}}^{2} = \mathrm{W}_{2} * \mathrm{P}_{\mathrm{LOS}}^{2}$$

and so on, till the sets of data.

$$\mathrm{P}_{\mathrm{new}}^{n} = \mathrm{W}_{n} * \mathrm{P}_{\mathrm{LOS}}^{n}$$

With this separate calculated probability, total PLoS can be calculated. New PLoS is the sum of the probability of LoS collected from the different clusters.

$$P_{LOS}^{new} = P_{LOS}^{1} + P_{LOS}^{2} + P_{LOS}^{3} + \cdots + P_{LOS}^{n} \quad (57)$$

From the equation (57), the network availability can be derived.

5.3.2 Calculation of Network availability with AF relay

With the calculated probability of line of sight as given by 57, we can re-compute the network availability and make sure that we satisfy the system requirements. As the network availability is proportional to PLoS, the increase in the LoS will also increase the chances of the availability of the network to achieve 5 9's for the critical applications.

The approximated network availability as given by equation (41) can be re-written with the calculated PLoS,

$$\mathrm{P_A} \approx \Pr\{\alpha_{\mathrm{i}}^{1} \geq \alpha_{\mathrm{i}}^{\sim 1}\}\, \mathrm{P}_{\mathrm{LOS}}^{\mathrm{new}} \quad (58)$$

The total network availability in equation 44 becomes,

$$1 - P_A \approx (1 - P_{LOS}^{new}) + (1 - Pr\{\alpha_i^1 \geq \alpha_i^{\sim 1}\}) \quad (59)$$

Numerical results can be plotted with the above approximate and accurate network availability.

5.4 Simulation results of relay facilitated URLLC UAV system

As we have seen in the UAV simulation results of UAV-Assisted Uplink Transmission, it is hard to obtain good PLoS and network availability with a single mobile UAV. The below simulation results have proved that the implementation of a facilitated relay on top of the building can achieve the direct probability of LoS in most situations.

In this section, I have provided the simulation results that were obtained for the PLoS, the network availability after the implementation of relay.

5.4.1 Probability of LoS with AF relay

Figure 26 depicts the variation of PLoS versus the altitude of the UAV as given by equation (57) for the high-rise urban environment. We can observe that LoS reaches 1 even with low altitude. Hence it proves that AF relay on the corner of rooftop of high-rise or tall building enhances the performance of communication system.

Note:
This has been implemented only for high-rise, it can also be implemented for other environmental conditions such as dense urban and urban to increase the LoS.

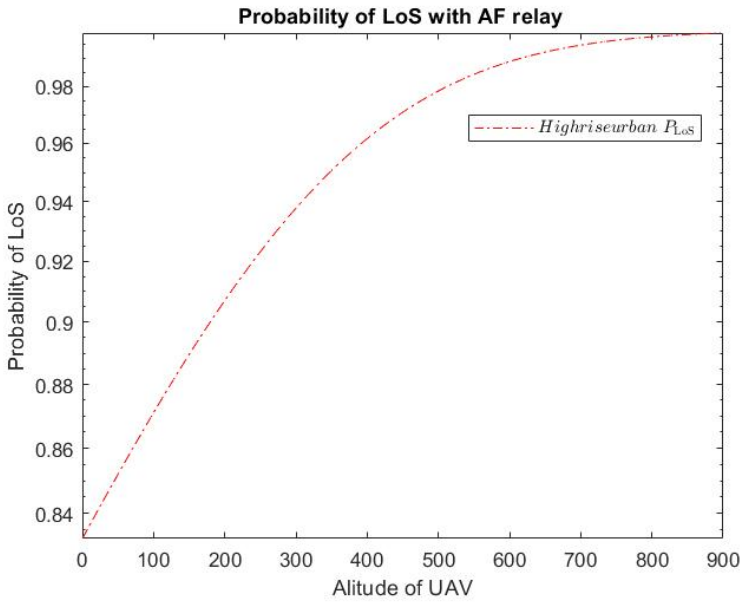

Figure 26 PLoS after AF relay implementation

5.4.2 Network availability with AF relay

Figure 27 represents the network availability after the implementation of AF relay for a high-rise urban environment. This graph has been plotted with the equations 58 and 59 for accurate and approximate network availability, respectively. We can notice that both probabilities reach the maximum with the use of an AF relay.

Therefore, it highly satisfies the latency and reliability requirement for URLLC and critical applications.

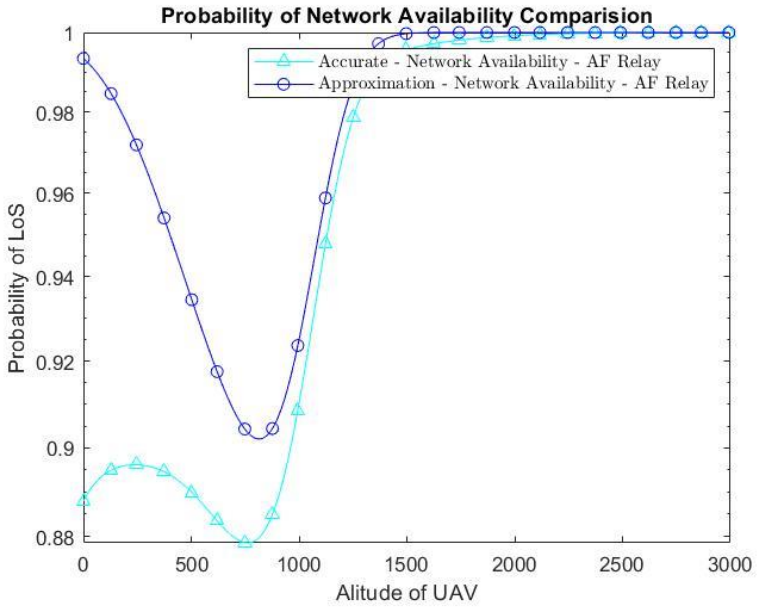

Figure 27 Network availability after the implementation of AF relay

Thus, this chapter explains the proposed idea on the implementation of relay on the side of the rooftop of a building. We can observe from the simulation that we are able to achieve the PLoS and network availability.

6 Numerical Results and Simulations comparison

This chapter contains the calculations and assumptions performed for modelling the system and the comparison of simulation before and after relay.

6.1 System parameters

In table 7, I have mentioned the considered or predefined values for certain parameters that are used in the simulation for MATLAB [1] .

Table 7 System Parameters

Notation	Value
Minimum Altitude of UAV	5m
Maximum Altitude of UAV	1500m
Packet size	32 bytes
Carrier frequency	2 GHz
Single-sided noise spectral density	-174DBm/Hz
Network availability requirement	99.999%
Transmit power	23 dBm
Required packet loss probability	10^{-7}
Transmission delay	0.5 ms
Bandwidth	5 MHZ

6.2 Channel parameters

The tables 8 and 9 summarizes the ITU-R parameters for different environments [16] and the channel parameters [1].

Table 8 ITU-R parameters for different environments

Environment	α	β	γ
Suburban	0.1	750	8
Urban	0.3	500	15
Dense Urban	0.5	300	20
Highrise Urban	0.5	300	50

Table 9 Channel Parameters

	Suburban	Urban	Dense Urban	Highrise Urban
ϕ	4.88	9.61	12.08	27.23
ψ	0.43	0.16	0.11	0.08
μ_0	0	0.6	1	1.5
μ_1	18	17	20	29
a_0	11.25	10.39	8.96	7.37
a_1	32.17	29.6	35.97	37.08
c_0	0.06	0.05	0.04	0.03
c_1	0.03	0.03	0.04	0.03

6.3 Comparison of Simulation results before and after the relay

In this section, I have compared the simulation results of PLoS, the network availability before and after the implementation of relay.

6.3.1 PLoS comparison

Figure 28 depicts the variation of PLoS versus the altitude of the UAV as given by equation (6) and equation (57) for the high-rise urban environment. From the graph below, we can visualize the massive improvement in multi-UAV communication attained through AF relay. Comparing the curves of high-rise urban environment with that of high rise urban with AF relay it can be seen that a big difference in achieving the PLoS.

Interestingly, Buildings with heights as high as 3000 meters or 3 km are never reaching probability ‘1’ whereas, buildings with AF relays reach probability ‘1’ with heights of around 2000 meters. Thus, it is correct to infer that relays undoubtedly build up the performance of the communication system especially when we have a variation in the building height or environment where a tall building is present.

As relays are cost-effective, we can also implement the idea of a relay in other important critical applications like the internet of things.

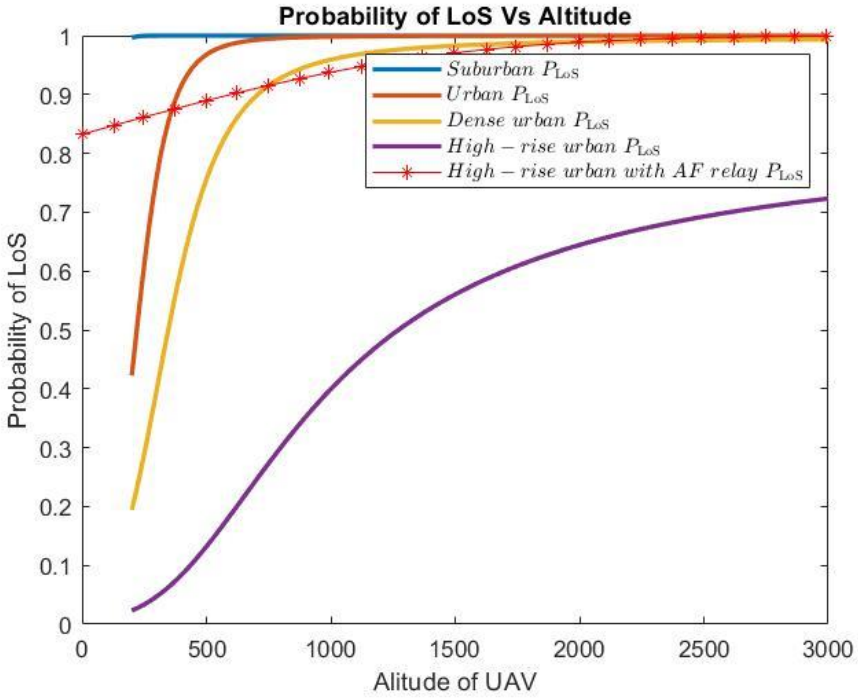

Figure 28 PLoS comparison before and after AF relay

It is important to notice that the suburban always reaches the PLoS irrespective of the building height. Therefore, it is not necessary to consider suburban, whereas it can be very useful for other environmental conditions.

6.3.2 Network availability comparison

Figure 29 depicts the variation of probability versus the altitude of the UAV with and without a relay. In the case of a single UAV, we used the equation (41) and equation (44) for accurate and approximate network availability, respectively. Whereas the implementation of the relay has been plotted with the equations (58) and (59) for accurate and approximate network availability, respectively.

We can observe that in the case of 'no relay', as there are many interference or obstacle in the system, there is a huge lag in the curve. Whereas in the case of 'with relay', there is not much lag in the system performance because it overcomes the interference by fixing the relay on the rooftop. Hence it can be proven that the AF relay enhances the performance of UAV.

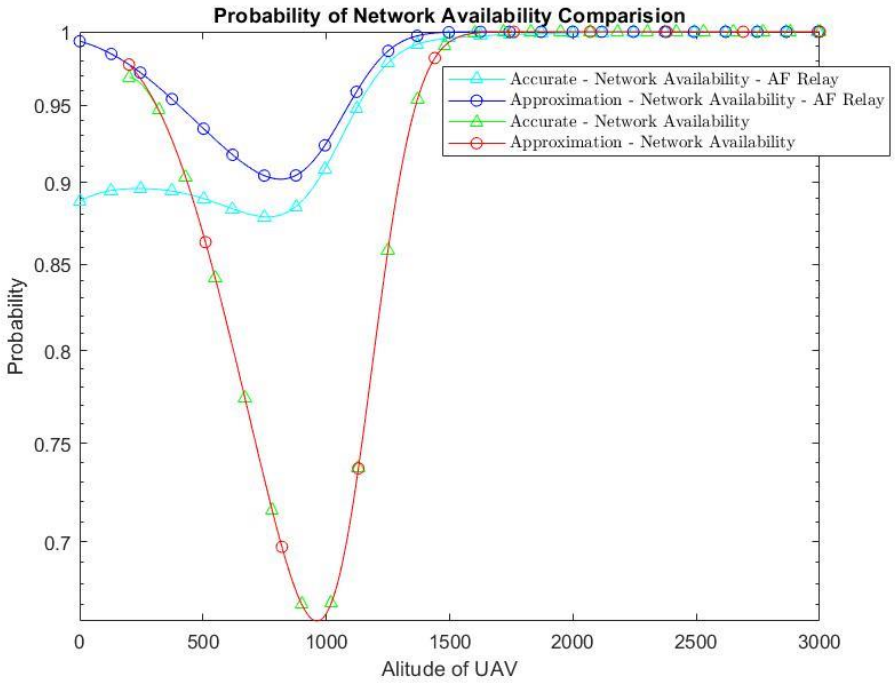

Figure 29 Network Availability comparison

Hence, facilitated relay in URLLC is the best for the wireless communication systems.

7 Conclusion and Scope of the thesis

In my thesis, we have explored and covered the important concepts of the 5G, URLLC, UAV, and its applications, wireless channel model, ground to air path loss model, and the delay analysis. To meet the strict URLLC constraints, improvements can be made on each of the three dimensions: reducing latency directly, increasing reliability and availability. We have exploited few techniques to improve the probability of LoS. The total SNR, the rate, overall network availability, and the overall BER have also been derived and optimized.

In the UAV-Assisted Uplink Transmission, we have a single mobile UAV, which acts as the mediator between the transmitter and the destination to avoid the interference, diffractions that block the direct transmission. We have also found an efficient algorithm to optimise the UAV altitude and the bandwidth that scales linearly with the geographical scale of the different environments.

Even with a single mobile UAV, it is difficult to establish a stable data link when obstacles such as trees, tall buildings, or mountains separate UAV and GCS, especially in the high-rise urban scenario. To harness the advantages of UAVs in these situations and minimize the drawbacks at the same time, an alternative solution is to deploy a multi-UAVs system, which could utilize the inter-connectivity to maintain uninterrupted communication with GCS. The use of a communication relay system provides a practical way to solve these problems, improving the performance of UAV communication when there is NLoS.

My thesis work primarily focused on evaluating the impact of placing an amplify and forward relay between the transmitter and the mobile UAV. We have worked on the optimal UAV positioning problem for both the mobile UA and the relayed UAV in different environments such as urban, dense urban, and high-rise urban.

To place the relay on the corner of the rooftop of a building, the real-time distribution of building heights was taken and used. Based on the data collected, the average height of the building for different environments is calculated and taken as the new ground level. The distribution of the building heights has been grouped as per different environment height. Once the data is finalised on the building height, the AF relay can be fixed.

Simulation results have shown the massive positive impact on the probability of LoS and network availability graphs. Thereby, the URLLC system requirements for the emergency and the critical requirements using the unmanned aerial vehicle with AF relay can be fully achieved.

7.1 Future work

- The proposed system works on maximising the coverage by increasing the LoS and optimising the altitude. We shall propose an efficient deployment method that not just maximises the coverage but also ensure that the coverage areas of UAVs do not overlap. We have not focused on the interference part; this can be our future scope.

- To reap the benefits of UAV-enabled wireless systems, flight time considerations need to be considered. Since the battery of the UAV cannot stay longer in the sky, we need to also focus on the replacement of the UAV or to power the UAV when the battery gets lower. Energy efficiency becomes a very critical challenge. Some studies have studied energy efficiency, these studies remain largely limited in scope as they do not analyse the interplay between energy efficiency and wireless communication performance. In any case, we must optimize the performance of UAV-enabled wireless systems under the energy and flight time constraints of UAVs.

- We have explored the use of amplifying and forward relay. The scenario can also be explored with the use of decode and forward protocol, which decodes the message which might be useful to reduce the error constraints.

- Our study does not consider practical factors, such as wind effects, heading, gyro, or acceleration. They can change the distance between transmitter and receiver and hence, affect the performance. However, they are beyond the scope of this research.

- We can explore to have the different antennas such as MIMO, isotropic and directional and choose according to the environmental, terrain and analyse the performance of the system.

- The co-existence of aerial base stations with terrestrial cellular networks needs to be explored as well. While designing the UAV-assisted cellular networks, several fundamental trade-offs need to be considered. For instance, the overall network performance can be improved by intelligent mobility of UAVs, however, it is limited by the capabilities of the UAVs and can lead to a significant UAVs' energy consumption.

8 Bibliography

[1] C. She, C. Liu, T. Q. S. Quek, C. Yang, and Y. Li, "UAV-Assisted uplink transmission for ultra-reliable and low-latency communications," *2018 IEEE Int. Conf. Commun. Work. ICC Work. 2018 - Proc.*, no. May, pp. 1–6, 2018, doi: 10.1109/ICCW.2018.8403626.

[2] C. She, C. Liu, T. Q. S. Quek, C. Yang, and Y. Li, "Ultra-reliable and low-latency communications in unmanned aerial vehicle communication systems," *IEEE Trans. Commun.*, vol. 67, no. 5, pp. 3768–3781, 2019, doi: 10.1109/TCOMM.2019.2896184.

[3] G. J. Sutton *et al.*, "Enabling Technologies for Ultra-Reliable and Low Latency Communications: From PHY and MAC Layer Perspectives," *IEEE Commun. Surv. Tutorials*, vol. 21, no. 3, pp. 2488–2524, 2019, doi: 10.1109/COMST.2019.2897800.

[4] H. Alves and J. Nielsen, "Machine-type Communications: from massive connectivity to ultra- reliable low latency communication," 2018.

[5] 5G Americas white paper Nov 2018, "New services and applications with 5G URLLC," *New Serv. Appl. with 5G URLLC*, vol. 57, no. 2, pp. Contents2–Contents2, 2018, doi: 10.3143/geriatrics.57.contents2.

[6] S. Schiessl, J. Gross, and H. Al-Zubaidy, "Delay analysis for wireless fading channels with finite blocklength channel coding," *MSWiM 2015 - Proc. 18th ACM Int. Conf. Model. Anal. Simul. Wirel. Mob. Syst.*, pp. 13–22, 2015, doi: 10.1145/2811587.2811596.

[7] C. She, C. Yang, and T. Q. S. Quek, "Radio Resource Management for Ultra-Reliable and Low-Latency Communications," *IEEE Commun. Mag.*, vol. 55, no. 6, pp. 72–78, 2017, doi: 10.1109/MCOM.2017.1601092.

[8] Mohammad Mozaffari, "Wireless Communications and Networking with Unmanned Aerial Vehicles : Fundamentals , Deployment , and Optimization," no. 23, 2018.

[9] Y. Zeng, R. Zhang, and T. J. Lim, "Wireless communications with unmanned aerial vehicles: Opportunities and challenges," *IEEE Commun. Mag.*, vol. 54, no. 5, pp. 36–42, 2016, doi: 10.1109/MCOM.2016.7470933.

[10] A. Al-Hourani, S. Kandeepan, and S. Lardner, "Optimal LAP altitude for maximum coverage," *IEEE Wirel. Commun. Lett.*, vol. 3, no. 6, pp. 569–572, 2014, doi: 10.1109/LWC.2014.2342736.

[11] R. J. Kerczewski and James H.Griner, *Control and non payload communications link for integrated unmanned aircraft operations*. .

[12] M. Azari, "Wireless Communications with Unmanned Aerial Vehicles (UAVs)," no. September, 2019.

[13] M. Mozaffari, W. Saad, M. Bennis, Y. H. Nam, and M. Debbah, "A Tutorial on UAVs for Wireless Networks: Applications, Challenges, and Open Problems," *IEEE Commun. Surv. Tutorials*, vol. 21, no. 3, pp. 2334–2360, 2019, doi: 10.1109/COMST.2019.2902862.

[14] G. Durisi, T. Koch, and P. Popovski, "Toward Massive, Ultrareliable, and Low-Latency Wireless Communication with Short Packets," *Proc. IEEE*, vol. 104, no. 9, pp. 1711–1726, 2016, doi: 10.1109/JPROC.2016.2537298.

[15] W. K. Jenkins and B. Dig-, "Discrete-Time Signal Processing Blocklength."

[16] A. Al-Hourani, S. Kandeepan, and A. Jamalipour, "Modeling air-to-ground path loss for low altitude platforms in urban environments," *2014 IEEE Glob. Commun. Conf. GLOBECOM 2014*, pp. 2898–2904, 2014, doi: 10.1109/GLOCOM.2014.7037248.

[17] B. Li, Y. Jiang, J. Sun, L. Cai, and C. Y. Wen, "Development and testing of a two-UAV communication relay system," *Sensors (Switzerland)*, vol. 16, no. 10, 2016, doi: 10.3390/s16101696.

[18] A. Ranjha and G. Kaddoum, “Quasi-Optimization of Distance and Blocklength in URLLC Aided Multi-Hop UAV Relay Links,” *IEEE Wirel. Commun. Lett.*, vol. 9, no. 3, pp. 306–310, 2020, doi: 10.1109/LWC.2019.2953165.
[19] H. Ren, C. Pan, K. Wang, W. Xu, M. Elkashlan, and A. Nallanathan, “Joint Transmit Power and Placement Optimization for URLLC-Enabled UAV Relay Systems,” *IEEE Trans. Veh. Technol.*, vol. 69, no. 7, pp. 8003–8007, 2020, doi: 10.1109/TVT.2020.2992736.
[20] C. G. Tsinos, S. Chatzinotas, and B. Ottersten, “Hybrid Analog-Digital Transceiver Designs for mmWave Amplify-and-Forward Relaying Systems,” *2018 41st Int. Conf. Telecommun. Signal Process. TSP 2018*, no. May, 2018, doi: 10.1109/TSP.2018.8441203.
[21] Y. Chen, W. Feng, and G. Zheng, “Optimum Placement of UAV as Relays,” *IEEE Commun. Lett.*, vol. 22, no. 2, pp. 248–251, 2018, doi: 10.1109/LCOMM.2017.2776215.
[22] J. Chen and D. Gesbert, “Optimal positioning of flying relays for wireless networks: A LOS map approach,” *IEEE Int. Conf. Commun.*, 2017, doi: 10.1109/ICC.2017.7996921.

Image Reference:

[23] https://www.vamsitalkstech.com/architecture/the-four-key-5g-architecture-principles/

[24] https://www.sciencedirect.com/topics/engineering/blocklength